Understanding the Relationship Between Ecdysone Signaling and the Lipin Protein in *Drosophila melanogaster*

by

Helen Gloege

A Paper Presented to the

Faculty of Mount Holyoke College in

Partial Fulfillment of the Requirements for

The Degree of Bachelors of Arts with

Honor

Department of Biological Science

South Hadley, MA 01075

May 2023

This paper was prepared

Under the direction of

Professor Craig Woodard

For eight credits

ACKNOWLEDGEMENTS

Firstly, I would like to thank Mount Holyoke for providing me with this opportunity. I would like to thank the Mount Holyoke Biological Sciences department for their resources and support.

I am incredibly grateful to my advisor Craig Woodard for taking a chance on me and for providing me with the opportunity to pursue research. I appreciate your enthusiasm and support in my research.

Thank you to Professors Sarah Bacon and Ken Colodner for agreeing to serve on my thesis committee and for allowing me to come to you with questions and providing excellent advice.

Thank you to the Woodard lab for your support and assistance. I enjoyed working alongside you to learn experimental procedures and talking science. Thank you to Ceren Citak and Lauren Comeau for our fly food cooking and chatting sessions.

I would also like to thank my friends Zoe Hellman, Catelyn Fitzgerald, and Ellen Switchenko for your love and support and allowing me to ramble about biology and helping me build confidence in myself and my work. Thank you also to Kristen Johnson for your incredible support as my thesis buddy and editor, I couldn't have done it without you. Thank you to Google Scholar for allowing me to discover Lipin. Thank you also to the bands Bastille and Rise Against for keeping me company in the lab late at night.

Thank you to my family for supporting me in my college journey and pushing me to pursue science research. While I know you often didn't understand what I was talking about, I appreciate your enthusiasm and encouragement. I wouldn't be here without your support.

Finally, I would like to thank all of the Professors I have had here and had the privilege to take classes with.

TABLE OF CONTENTS

LIST OF FIGURES

Page

LIST OF TABLES

ABSTRACT

Drosophila melanogaster, the common fruit fly, undergoes four major stages of development: embryonic stage, larval stage, pupal stage, and adult stage. During the larval stage, individuals increase in size and consume nutrients, which are then stored in the cells of the fat body. When the larva reaches critical weight, the formation of the pupal case or pupariation occurs over four days and undergoes a transformation from its larval form to its adult form. During these four days, the pupa will not consume any external nutrients and is reliant on the nutrients stored in the cells of the fat body as a result. The pupal stage is an energetically expensive process.

In *Drosophila*, there is a single *lipin* gene orthologue known as *dLipin*. Lipin is a protein that is encoded by the *lipin* gene. Lipin is considered essential for normal adipose tissue development and triacylglycerol (TAG) storage. *dLipin* is linked to energy metabolism and is considered to be crucial under nutrient deprivation conditions. *dLipin* also plays a role in insulin sensitivity in the larval fat body (Lehmann, 2018). Ecdysone is a steroid hormone that acts through a receptor to regulate the transcription of specific target genes. This steroid hormone is the central regulator of developmental transitions in *Drosophila* and leads to pupariation at the beginning of metamorphosis. I hypothesize that ecdysone signaling activates the transcription of the *dLipin* gene during metamorphosis.

To test this hypothesis, I am using the wild-type genotype as a control, and *Cg-Gal4; UAS-EcR-DN* flies as an ecdysone-signaling-deficient experimental genotype. Results of the Real-Time Quantitative Polymerase Chain Reaction (qRT-PCR) indicate the opposite of the hypothesis and that ecdysone signaling instead inhibits the transcription of the *dLipin* gene. Ecdysone deficient *Drosophila* resulted in up-regulation of *dLipin* compared to the wild-type *Drosophila*. Studying lipin in the *Drosophila* model will help lead to an understanding of the basic function of lipin in metazoans and lipin's role in fat cell function and energy metabolism (Schmitt, 2015).

INTRODUCTION

Metabolism

There are multiple signaling pathways that control metabolism. Many of these pathways are conserved between mammals and *Drosophila melanogaster,* including those controlled by nutrients, steroid hormones, glucagon, and hedgehog (Lehmann, 2018). In *Drosophila* and other animals, neutral fats and triacylglycerols (TAGs) are used to store chemical energy for later use. TAGs are cytoplasmic lipid droplets stored in a compact formation (Lehmann, 2018). TAGs are the primary energy stores in *Drosophila* and are located in the fat body. TAGs are important for survival during periods of starvation and metamorphosis.

Neutral fats are broken down by lipases and the fat breakdown is controlled by proteins from the perilipin family (Lehmann, 2018). Perilipins are proteins that coat lipid droplets in fat-storing cells. They are not essential under normal feeding conditions (Lehmann, 2018). TAGs are broken down through hydrolysis of their ester bonds by lipases. (Heier & Kuhnlein, 2018).

Drosophila, similar to other organisms, relies on external signals and the availability of nutrients to control the growth of the entire organism. In *Drosophila*, the organism's growth is controlled through the fat body (Colombani *et al*, 2003). The fat body works with additional pathways to serve as a nutrient sensor that can also restrict growth. The control of organismal growth is run through the target of rapamycin (TOR) signaling pathway and the inhibition of growth occurs through the phosphoinositide 3-kinase (PI3K) signaling pathway

(Colombani *et al*., 2003). TOR signaling is associated with sensing internal nutritional status and also promotes translation to increase ribosomal activity (Koyama *et al*., 2020). PI3K signaling is known as a regulator of cell growth and also has different functions during development. There is a mechanism that is set off by amino acid availability that comes from the fat body to cause growth in larvae, with amino acid deprivation causing restricted growth of larval tissues (Colombani *et al.*, 2003). If larvae don't have enough access to food, the lack of food will affect their adult body size with resulting decreased body size or delays in metamorphosis (Colombani *et al.*, 2003).

Drosophila melanogaster

Drosophila melanogaster, more commonly known as the fruit fly, is a model organism used to study a wide range of biological processes. *Drosophila* are commonly used because of their short life cycle as it takes only about 10 days for a fertilized egg to grow into an adult fly. They are also very small and easy to maintain in large quantities. *Drosophila* has only four pairs of chromosomes, which helps in mapping genes. The entire genome of *Drosophila* has been sequenced and annotated.

An increasing number of studies have used the organism to understand signaling pathways that control metabolism as there are many functionally conserved elements between mammals and *Drosophila* (Lehmann, 2018). Using

Drosophila has allowed researchers to fill in the gaps and find new parts of signaling pathways and networks.

Drosophila metamorphosis

The life cycle of *Drosophila* consists of four major stages, embryo, larvae, pupa, and adult. The larval stage includes the first, second, and third instars. The *Drosophila* begins life as a fertilized egg and undergoes embryogenesis for the first 24 hours. The first instar larva develops and immediately begins feeding, and after a day will molt to become the second instar larva. The second instar larvae burrows into the food source, and when the third instar is mature, it leaves the food and searches for a place for pupariation (Fernández-Moreno *et al.*, 2016). The first instar and second instar stages each take about 24 hours to complete. The third instar stage takes about 48 hours. During this time the larvae continuously eat and grow in size. *Drosophila's* mass increases approximately 200-fold during this larval stage (Grewal, 2012).

During metamorphosis the third instar larva forms a pupal case (puparium) and begins metamorphosis and emerges as an adult. The transition from larva into pupa is induced by critical weight. *Drosophila* commits to releasing prothoracicotropic hormone (PTTH), which triggers neuroendocrine signaling, which in turn leads to a maturation-inducing ecdysone pulse that initiates metamorphosis (Koyama *et al.*, 2020). During that time a number of the larval tissues are destroyed, and the larval fat body is remodeled. Before metamorphosis,

the larval fat body is a single-cell layer of white, translucent cells that form sheets of tissue. Individual fat cells are flat and polygonal in shape and are tightly associated with each other. The fat cells then begin to change and take on a rounder shape and begin to disaggregate from each other. The fat body cells then become spherical and detach from each other. The detached fat cells remain present throughout metamorphosis and are still present in the newly eclosed adults (Nelliot *et al*., 2006).

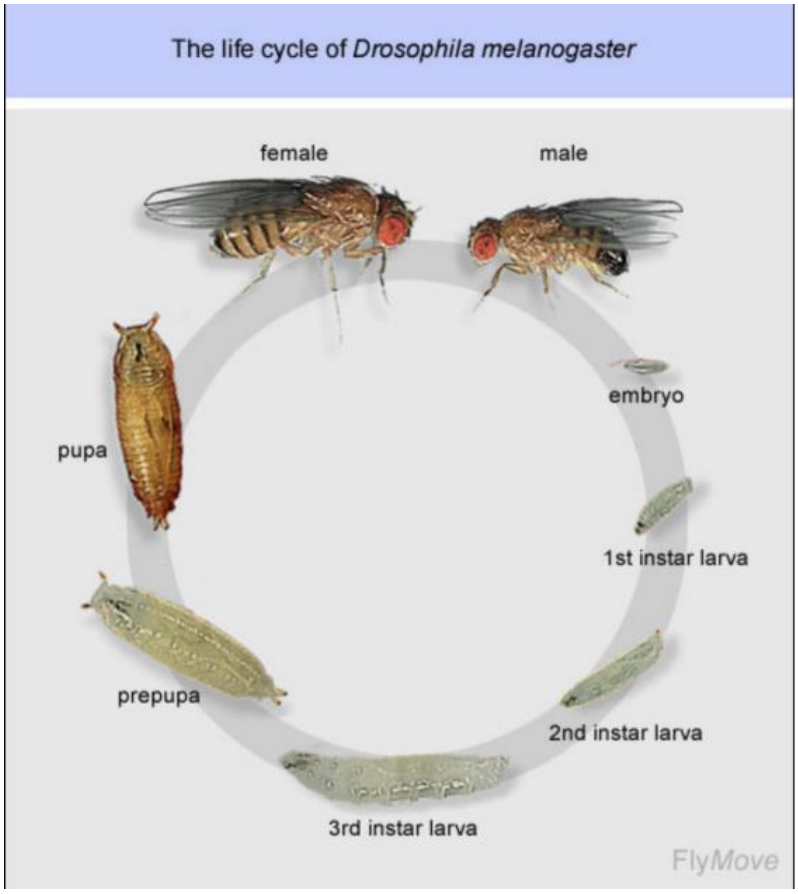

Figure 1. Life cycle of *Drosophila melanogaster*. The life cycle is broken down into four main stages: embryo, larva, pupa, and adult. The life cycle lasts about 12 days at 25℃. (Adapted from Weigmann *et al*., 2003)

Metabolism during metamorphosis

During the process of metamorphosis, *Drosophila* does not consume an external source of energy. They must rely on stores of fat that were built up during the larval stage. When the *Drosophila* commits to metamorphosis, the amount of CO_2 released per hour is high and begins to drop, reaching a low point and then increasing the amount of CO_2 released per hour again, following a U-shaped metabolic curve (Merkey *et al*., 2011). During the first 24 hours of metamorphosis there is a loss in metabolic rate that evens out around 24 hours into metamorphosis and remains low for the next 48 hours and will then increase as the pupae gets closer to eclosion at around 96 hours into metamorphosis (Merkey *et al.,* 2011). Merkey *et al.* (2011) discovered that metamorphosis is a costly process resulting in 35% of initial lipid stores and 27% of initial carbohydrate stores consumed.

Ecdysone

20-hydroxyecdysone is a steroid hormone that acts in *Drosophila melanogaster* through pulses that lead to developmental transitions in the life cycle of the organism (Colombani *et al*., 2005). This paper will refer to 20-hydroxyecdysone by the shorter name of ecdysone. Ecdysone is secreted in the *Drosophila's* prothoracic glands, a pair of endocrine glands that are part of the ring gland (Kannangara *et al*., 2021). Ecdysone works by activating the nuclear

ecdysone receptor complex in target tissues. The receptor complex binds to ecdysone-response elements and causes expression of ecdysone target genes that lead to developmental transitions (Kannangara *et al*., 2021). Ecdysone has also been found in the haemolymph, a fluid similar to blood in vertebrates that circulates inside of invertebrates, in an active form that peaks prior to molting and metamorphosis (Kannangara *et al.*, 2021).

Peaks of ecdysone titer control the timing of developmental transitions. Ecdysone works primarily through the fat body as the fat body will send the ecdysone signal to the larval tissues (Colombani *et al*., 2005). During the 3rd instar larval stage, three smaller ecdysone pulses followed by a larger pulse, assist in driving developmental progression (Koyama *et al*., 2020). The first ecdysone pulse controls critical weight and the second pulse induces glue production (Kannangara *et al*., 2021). The third smaller ecdysone pulse induces the larvae to stop feeding and move to find an appropriate pupariation site (Koyama *et al*., 2020; Kannangara *et al*., 2021). A larger ecdysone pulse causes the onset of pupariation (Kannangara *et al.,* 2021). A smaller pulse of ecdysone will occur at 10-12 hours after the puparium formation (Woodard *et al.*, 1994).

Ecdysone has numerous roles within the metamorphosis process. Ecdysones role includes a role in growth and patterning of adult tissues, eversion and proliferation of imaginal disc cells, apoptosis of larval cells, and restructuring of the nervous system (Kannangara *et al*., 2021). Inhibition of ecdysone signaling during the 3rd instar larvae has been known to result in lipid accumulation in the

fat body while not seeing an increase in the cell number (Kamoshida *et al*., 2012). This links ecdysone signaling with lipid mobilization in the fat body. The ecdysone receptor (*EcR*) induces the expression of a variety of target genes and processes that include control over lipid accumulation in the fat body (Kamoshida *et al*., 2012).

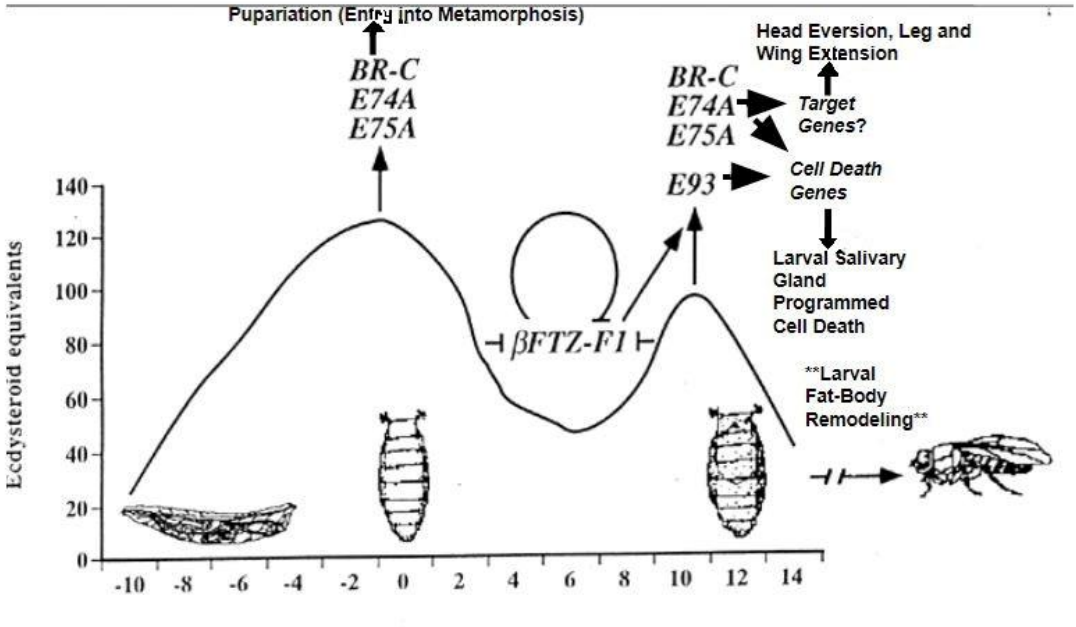

Figure 2. A representation of ecdysone pulses during early metamorphosis. Ecdysone peaks at about 0 hr APF and decreases hitting a low point around 6 hr APF and peaking again around 12 hr APF. (Adapted from Notarangelo, 2014)

Lipin in Vertebrates

In *Drosophila melanogaster*, there is a single lipin orthologue, *dLipin*. In addition to *dLipin*, lipin is present in other species with three orthologues in vertebrates other than fish, two orthologues in fish and plants, and one orthologue in nematodes, plasmodium, and yeast (Reue and Zhang, 2008). Research on lipin genes in different species has demonstrated that they are highly conserved (Han *et al.*, 2011). This indicates our understanding of lipin's role in *Drosophila* may also translate across species. Most vertebrate species have three *lipin* family genes known as *lipin-1*, *lipin-2*, and *lipin-3*, and most of the research has been conducted on *lipin-1*. *Lipin-1* is expressed in adipose tissue, skeletal muscle, and testis, and can localize to either the cytoplasm or the nucleus (Reue and Dwyer, 2009). *Lipin-2* is most prominently expressed in the liver and brain and *lipin-3* is present at low levels in various tissues, the small intestine, and liver (Reue and Zhang, 2008). *Lipin-1* is also known to form hetero-oligomers with *lipin-2* and *lipin-3* (Harris and Finck, 2011).

Lipins are considered to be regulators of lipid metabolism and have the ability to move around the cell and play multiple roles (Harris and Finck, 2011). During development of mature adipocytes, *lipin-1* is found to be expressed between 10 to 20 hours after induction of differentiation and is again induced at 2 days after induction (Reue and Zhang, 2008). Studies done in mice where lipin is removed have resulted in low phosphatidic acid phosphatase (PAP) activity in fat,

brain, kidney, lung, cardiac and skeletal muscle, and a 50% reduction in liver (Harris and Finck, 2011). PAPs are enzymes that play a role in lipid homeostasis. In *lipin-1* deficient mice with low PAP activity, Schwann cells were found to be affected with peripheral neuropathy associated with myelin degradation and attenuated nerve conduction velocity (Reue and Dwyer, 2009). However, it is unclear if this translates to humans.

On the other hand, when lipin levels are increased in adipose tissue or skeletal muscle, there are studies that have found that it will promote obesity (Phan and Reue, 2005). Changes in lipin levels cause dramatic shifts in adiposity which can result in lipodystrophy or obesity in the mouse model (Phan and Reue, 2005). However, mutations in *lipin-1* in humans aren't associated with lipodystrophy (Harris and Finck, 2011). Lipin has been indicated to govern energy expenditure and fatty acid utilization in mice studies (Phan and Reue, 2005).

Lipin-1 may play a role in directing nutrients toward energy storage or utilization and is a downstream target of mammalian TOR or mTOR (Reue and Zhang, 2008). *Lipin-1* is found to play a role in increased phospholipid synthesis for ER membrane expansion that occurs as B lymphocytes differentiate into antibody-secreting plasma cells (Reue and Zhang, 2008). Lipin levels are implicated in skeletal muscles as determinants of energy expenditure and fatty acid utilization, similar to their role in *Drosophila* (Phan and Reue, 2005). Lipin

overexpression in muscles led to obesity-associated insulin resistance (Phan and Reue, 2005).

In people, *lipin-1* and *lipin-2* mutations are associated with human disease (Reue and Dwyer, 2009). *Lipin-1* is connected to muscle metabolism and its expression is found to be higher in conditions that cause muscle atrophy (Reue and Zhang, 2008). Similar to *dLipin*, there is a link between *lipin-1* and insulin sensitivity found in mouse and human studies (Reue and Zhang, 2008). *Lipin-1* is found to contain at least 19-23 sites that are phosphorylated in response to insulin (Harris and Finck, 2011). With *lipin-1* mRNA levels in adipose tissue are inversely correlated with glucose, insulin, and insulin resistance (Reue and Zhang, 2008). More specifically *lipin-1* mRNA expression is regulated during adipocyte differentiation and in liver during fasting and in type 1 and type 2 diabetes mellitus (Reue and Zhang, 2008). *Lipin-1* also has a role as a transcriptional coactivator that promotes fatty acid oxidation (Reue and Dwyer, 2009).

Polymorphisms in the *lipin-1* gene *LPIN1* are associated with insulin levels and BMI in dyslipidemic families, as determined in a Finnish case study (Reue and Zhang, 2008). Polymorphisms have also been associated with other traits such as insulin and glucose levels, resting metabolic rate, and systolic blood pressure (Reue and Dwyer, 2009). Phan and Reue (2005) argue that the *LPIN1* gene may be a candidate for disorders associated with decreased and increased adipose tissue mass. Mutations in *LPIN1* have also been found in patients with

recurrent acute myoglobinuria in childhood (Reue and Dwyer, 2009). Myoglobinuria is the presence of excess myoglobin in the urine that is generally caused by muscle breakdown and can lead to kidney injury.

Lipin-2 mutations in the *LPIN2* gene are specifically associated with Majeed syndrome. Majeed syndrome is an inflammatory disorder in humans that is characterized by sterile osteomyelitis, cutaneous inflammation, and dyserythropoietic anemia (Reue and Dwyer, 2009). Majeed syndrome is exceedingly rare with only twenty four documented cases.

dLipin

In *Drosophila melanogaster*, there is a single lipin orthologue, *dLipin*. *dLipin* is considered essential for normal adipose tissue development and triacylglycerols (TAG) storage. TAGs are principal energy stores in eukaryotic cells and also known as neutral lipids. Studies of lipin in *D. melanogaster* will lead to an understanding of the basic function of lipin in metazoans and lipin's role in fat body function and energy metabolism (Schmitt *et al*., 2015). The role of *dLipin* in the fat body of *Drosophila* has been examined via the analysis of loss-of-function mutations. Initial work on *Drosophila dLipin* has shown that *dLipin* loss-of-function during pupal development results in death during metamorphosis. The resulting dead pharate adults don't show obvious morphological defects although functions of the fat body were severely impaired

in *dLipin* mutants (Schmitt *et al*., 2015). When looking outside the fat body Schmitt *et al.* (2015) found that *dLipin* also played a role in other tissues, including the ovaries and imaginal discs. The larval salivary glands remained unaffected by *dLipin* loss-of-function. When Schmitt *et al.* (2015) looked at the cells themselves, they found that the nuclei of the cells were enlarged up to about 2-fold while some had undergone fragmentation. The nuclear fragmentation was determined to not have been caused by apoptosis. The fat droplets were also found to be much smaller. The cells were also found to have rounded and defective mitochondria and misshapen nuclear envelopes. The misshapen nuclear envelopes appeared shrunken or ruptured and the altered mitochondria tended to be round in shape and contained few cristae (Ugrankar *et al.,* 2011). The changes in mitochondria were visually similar to mitochondria in *Drosophila* cells undergoing apoptosis, which may indicate the fat body cells entered the apoptotic pathway (Ugrankar *et al*., 2011). When comparing the cells to cells in which p35, a gene that prevents apoptosis, had been knocked out, there was no clear difference in their nuclei (Ugrankar *et al*., 2011). When Ugrankar *et al*. (2011) inhibited apoptosis in the fat body, the defects still appeared, which indicates the defects aren't caused by the apoptotic pathway and are instead exclusively caused by *dLipin*. The data indicated that fat synthesis and fatty acid metabolism are disturbed.

Ugrankar *et al*. (2011) determined that the change in mitochondria and the impact of *dLipin* on mitochondrial function is similar to the role of *lipin-1* in the

vertebrate liver. The role of mitochondria dysfunction suggests an impact of *dLipin* on energy metabolism. *dLipin* transcript levels are upregulated under starvation conditions and the downregulation of *dLipin* and food withdrawal both lead to diminished starvation resistance.

In addition to being expressed in the larval fat body, *dLipin* is also expressed in the midgut and other regions of the gut, as well as the ring gland, ovaries, and imaginal discs (Ugrankar *et al.,* 2011). More specifically the staining done in the studies found *dLipin* was located in the cytoplasm and the nuclei of the cells while in malpighian tubules, the organs between the midgut and hindgut, the staining was located in the nuclei of the cells (Ugrankar *et al*., 2011).

Schmitt *et al*. (2015) further examined the role of insulin and the TORC1 pathway in relation to lipin. The results indicated that *dLipin* has an influence on signaling through the use of the InR-PI3K-Akt pathway. The study indicated that cells without *dLipin* have an impaired sensitivity to insulin in the fat body which may occur through the messenger PIP3 that is part of to PI3K or PTEN pathways (Schmitt *et al*., 2015). More specifically *dLipin* may have an impact on the activity of PI3K or PTEN in the pathway through PIP3. When p60, a regulatory subunit of PI3K was overexpressed it led to a reduction in *dLipin* which indicates that PI3K is required for *dLipin* activity and expression (Schmitt *et al*., 2015). Schmitt *et al*. (2015) concluded that *dLipin* likely has an essential role in maintaining sensitivity to insulin in the larval fat body but this likely doesn’t

apply to other tissues. The insulin-like receptor (InR) is believed to control *dLipin* function, similar to how it does in mammals with *lipin-1,* which undergoes phosphorylation in response to insulin (Schmitt *et al*., 2015). Given the importance of the InR pathway and PI3K as explained above, *dLipin* likely involves the InR-PI3K pathway. It is likely that the InR-PI3K-Akt pathway controls *dLipins* effect on cell growth (Schmitt *et al*., 2015). This role means that *dLipin* likely contributes to sensing insulin sensitivity but not insulin signaling. This is backed up by tissues without lipin demonstrating insulin resistance (Lehmann, 2018).

Schmitt *et al*. (2015) provides further evidence for the role of *dLipin* in insulin sensitivity through PAP activity. Lipins can convert phosphatidic acid into diacylglycerol as phosphatidate phosphatases or PAPs (Hood *et al*., 2020). PAP activity is considered a key regulatory enzyme in lipid metabolism (Ugrankar *et al*., 2011). They determined that decreased insulin pathway activity is caused by a loss of PAP activity caused by *dLipin* (Schmitt *et al*., 2015). *dLipin* has an effect on the glycerol-3 phosphate pathway and can cause changes in metabolites and will influence insulin sensitivity through intracellular changes. They also found that *dLipin's* phosphatidate phosphatase (PAP) activity is required for development beyond embryonic and early larval stages as well as potentially embryogenesis (Hood *et al*., 2020). The paper also determined translocation of *dLipin* after reducing TORC1 activity. The lack of TORC1 in the fat body leads to a systemic growth defect, whereas decreasing *dLipin* in the fat

body didn't affect organismal growth. TORC2 was not explored in this paper but may have a relation to *dLipin*. When combined, the reduction of *dLipin* didn't affect the growth of animals that lacked TOR. TOR likely has an influence on *dLipin's* ability to function in fat body development and fat storage (Schmitt *et al*., 2015). TORC1 is likely to control nuclear translocation of *dLipin,* however it is unclear how this pathway works as when InR and PI3K were reduced, there wasn't a nuclear translocation of *dLipin* (Schmitt *et al*., 2015). This research indicates that lipin plays a role in multiple pathways including those that involve insulin signaling. Insulin and TORC1 are different aspects of hormone production that occur in the ring gland.

Data suggests lipins are vital under starvation conditions (Lehmann, 2018). Hood *et al.* (2020) determined that lipin appears to have functions outside of just the fat body and in other parts of the body including the gut, the Malpighian tubules, the brain, and the endocrine ring gland. In the studies experiments on starvation conditions it appeared that lipin contributed to changes in feeding behavior produced by starvation conditions (Hood *et al*., 2020). Lipin is also known to move around the cell and lipins ability to move to the cell nucleus was essential under nutrient deprivation conditions. Lipin's impact on nuclear localization differed based on the tissue in the fed state. Nuclear translocation is regulated by the TOR pathway. In the gut and brain lipin showed partial nuclear localization whereas in the Malpighian tubules, lipin showed preferential nuclear localization (Hood *et al*., 2020). The ability of lipin to move

into the cell nucleus is important under nutrient deprivation conditions. Specific nutrients are believed to have a particular impact on nuclear translocation. When nutrients are scarce, lipin tends to translocate to the nucleus (Lehmann, 2018).

dLipin is upregulated during starvation conditions (Hood *et al*., 2020; Ugrankar *et al*., 2011). Schmitt *et al*. (2015) found evidence for lipins regulating genes to promote the use of fat stores during starvation conditions. Hood *et al*. (2020) also demonstrated that lipin is involved in immune response genes and may mediate or block genomic effects of certain nutrients.

Signaling pathways: TOR

Target of rapamycin or TOR signaling is a pathway that responds to cellular levels of amino acids and ATP (Baker and Thummel, 2007). TOR signaling is known to work with the insulin pathway to use the nutrient status of the animal to cause changes in cellular physiology that are associated with growth, translation, and autophagy (Baker and Thummel, 2007). More specifically, TOR can be activated by nutrients, specifically amino acids, or by insulin or other growth factors (Lehmann, 2018). Given its link to nutritional status, TOR is found to be reduced during starvation conditions (Baker and Thummel, 2007; Colombani *et al*., 2003).

In *Drosophila* TOR homolog (dTOR), dTOR is required for growth and mutations show cellular and physiological responses similar to those seen with amino acid deprivation (Colombani *et al*., 2003; Zhang *et al*., 2000). TOR is also related to larval growth control and is specifically linked with the fat body (Colombani *et al*., 2003). Zhang *et al*. (2000) proposed that the primary function of dTOR is to promote cell growth with decreased proliferation as a secondary effect of the signaling pathway. dTOR is believed to be required for normal growth during larval development and cellular growth through activation of the PI3K signaling pathway (Zhang *et al*., 2000).

Signaling pathways: PI3K

The PI3K signaling pathway is activated by insulin signaling and provides a regulatory function for different systems including cellular metabolism, cell survival and fate decisions, as well as proliferation (Britton *et al*., 2002). The PI3K signaling pathway is in contact with the *Drosophila* insulin receptor known as Inr.

The Inr/PI3K signaling pathway is also associated with ecdysone production (Colombani *et al*., 2005). More specifically, The Inr/PI3K signaling pathway can activate ecdysone production (Colombani *et al*, 2005). Ecdysone signaling has been shown to downregulate PI3K signaling (Rusten *et al*., 2004).

When PI3K activity is reduced, it doesn't lead directly to cells that are not viable. However, when PI3K activity has been reduced in differentiated tissues in *Drosophila* larva, it has led to reduced cell growth and DNA replication (Britton *et al*., 2002). Given its link to insulin signaling, PI3K activity is believed to respond to nutritional conditions, yet InR/PI3K signaling isn't necessary for cellular growth and DNA replication (Britton *et al*., 2002; Colombani *et al*., 2003). In *Drosophila* starvation condition experiments, Inr/PI3K signaling hyperactivity was found to be fatal and downregulated Inr/PI3K activity was preferred to maintain metabolic homeostasis under starvation conditions (Britton *et al*., 2002).

Hypothesis

When *Drosophila* undergoes metamorphosis, the pupa does not consume any nutrients and relies solely on the stores they built up during the larval stage. The process of metamorphosis is energetically expensive, and the organism requires a certain amount of stored fat in order to survive metamorphosis. *dLipin* plays an important role in lipid and energy metabolism. Specifically, *dLipin* is upregulated under starvation conditions. Given *dLipin's* role in fat storage and in nutritionally-restrictive conditions and the need for fat storage release and nutritional restriction during metamorphosis when ecdysone is most active, there

must be an interaction between the two. This project tests the hypothesis that ecdysone signaling activates transcription of the *dLipin* gene.

MATERIALS & METHODS

Experimental Design

The proposed hypothesis was tested using the *Drosophila melanogaster* genotypes from Bloomington *Drosophila* Stock Center 360, 9452, and 7011. Fly stock 3605 is referred to as w[1118]. Fly stock 9452 is w[*]; P{w[+mC]=UAS-EcR.A.F645A}TP2 or *UAS-EcR-DN*. And fly stock 7011 is w1118; P{Cg-GAL4.A}2 or *Cg-Gal4.* The *UAS-EcR-DN* genotype stands for UAS-Ecdysone Receptor-Dominant Negative. The w^{1118} genotype served as the wild-type control to examine the role of *dLipin* when ecdysone was present. The *Cg-Gal4* and *UAS-EcR-DN* genotypes were crossed to create a genotype where ecdysone-signaling-deficient.

The target dissection points were chosen based on ecdysone's titers. As established, the first large pulse of ecdysone occurs at 0 hours after puparium formation (APF). After the first pulse, the level of ecdysone will decline and reach a low point at 6 hrs APF. Then the second major pulse of ecdysone will occur at 12 hrs APF (See image 2). Therefore, this experiment used fat bodies dissected from 0 hr APF, 6 hrs APF, and 12 hrs APF. APF was determined when the *Drosophila* had committed to metamorphosis and was no longer moving around.

Drosophila Care

All flies were housed at 25˚ Celsius (C) at 50% humidity in plastic bottles and vials on a standard yeast-based *Drosophila* culture medium. Each of the fly types were housed in standard conditions in fly bottles with an adequate food supply. Flies were transferred onto fresh medium in fresh bottles every 4-10 days to prevent development of mites and to maintain healthy stocks.

Fly crosses

In preparation for virgin fly collection, bottles with many larvae and pupae were cleared of all adult flies. Cotton balls were added to the base of the bottles and covered the food. Bottles were incubated at 25˚ C or at 18˚ C. If they were stored at 25˚ C, the virgins were then collected within 8 hours and if they were stored at 18˚ C, then they were collected within 18 hours. Once collected, the flies were sexed and kept in separate male and female vials to prevent mating prior to the crosses. When at least 20 flies of each experimental condition were collected, the crosses were then performed. The *Cg-Gal4* males were then placed with the *UAS-EcR-DN* females and the *Cg-Gal4* females with the *UAS-EcR-DN* males and allowed to procreate. The cross will result in *Cg-Gal4; UAS-EcR-DN* progeny. Virgin flies were used as the female *Drosophila* will store sperm so a fly that has previously mated may result in an incomplete cross.

Gal4-UAS System

The *Gal4-UAS* system (Duffy, 2002) was used to produce the ecdysone-signaling-deficient *Drosophila*. The system separates the target gene from the transcriptional activator in two transgenic lines. In one line, the target gene, *EcR-DN* in this case, is regulated by an upstream activation sequence, *UAS*, which is a *Gal4*-binding site. Without the *Gal4* activator, the target gene is unable to be expressed. In the other line, the *Gal4* gene is present to produce *Gal4* proteins, but no target gene is activated. When the two lines are crossed, the resulting progeny is generated with the desired phenotypes. The target gene is activated in a specific tissue through mating with a tissue-specific *Gal4* driver.

The two lines in this study were the *cg-Gal4* and *UAS-EcR-DN* lines. The *cg-Gal4* gene encodes a fat-body-specific *Gal4* driver (Duffy, 2002). The other transgene, *UAS-EcR-DN* carries a regulatory sequence that drives the expression of an *EcR* mutant, *EcR-DN*. The *EcR-DN* mutant contains a point mutation that makes it unable to bind to an ultra-spiral protein, USP, and form an ecdysone receptor. Ecdysone then acts through the ecdysone receptor. Both of the transgenes are on chromosome 2 in the heterozygous first generation progeny, so the *cg-Gal4* and *UAS-EcR-DN* gene are on the same chromosome. The *Gal4* protein will initiate the transcription of the target gene, *EcR-DN*, by binding to the *UAS* enhancer. The mutant's inability to bind to the USP and create the ecdysone

receptor prevents ecdysone signaling cascade. Only the resulting F1 progeny will have the desired ecdysone-signaling-deficient effect.

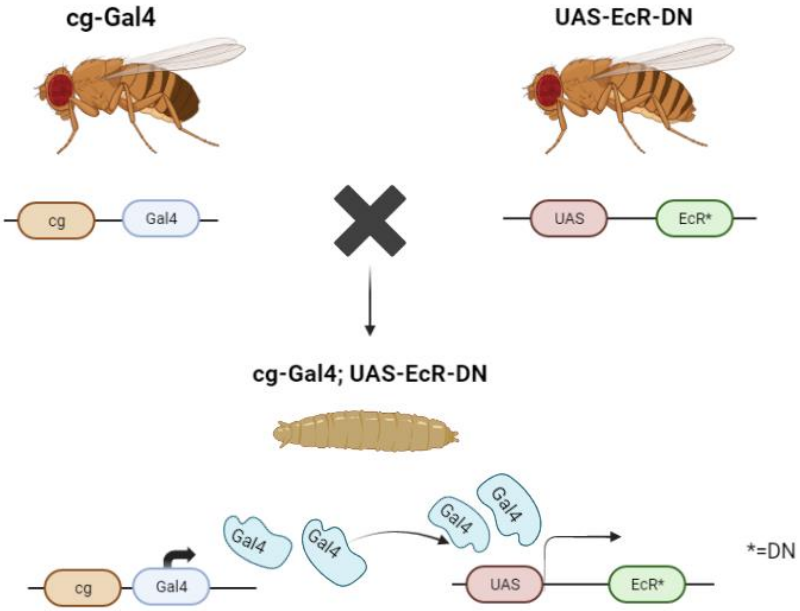

Figure 3. Visual of the *Gal4-UAS* system with the transgenes of *cg-Gal4* and *UAS-EcR-DN*. The two transgenes used in the study are *cg-Gal4*, a fat body specific gene, and *UAS-EcR-DN* (shown in cartoon as EcR*) carrying a loss-of-function mutant of the ecdysone-receptor transgene. The F1 progeny have both of the transgenes where the *Gal4* protein initiates the transcription of the target gene by binding to the *UAS* enhancer. This figure was made with BioRender.com.

Sample Collection

This project used both wild-type and *cg-Gal4*; *UAS-EcR-DN* flies. For each of the types of flies, 0, 6, and 12 hour prepupae were used. Five larvae of each type of fly and time were dissected, and the fat body removed and isolated within a sixty minute time frame. The isolated fat bodies are then placed in 30 µl of 1x phosphate buffer solution (PSB) using tweezers.

RNA Isolation

After the fat body was isolated and placed in a tube with the PBS, 300 µl of TRIzol reagent was added to the sample and the sample was then ground with a hand-held homogenizer. The sample was then frozen at -80˚ C for about twenty-four hours. The next day the sample was then warmed by hand, so the liquid was not frozen. Phase Lock Gel-Heavy 2 ml tubes were then pre-spun at 12,000 rpm for one minute. The contents were then added to the Phase Lock Gel-Heavy tube and 60 µl of chloroform was added. The tube was then capped and shaken for fifteen seconds by hand. The sample was then centrifuged at 12,000 rpm for ten minutes at 2-8˚C. After the centrifugation was finished, the tube was evaluated to determine if the phasing had separated the clear, aqueous phase and the phenol-chloroform phase and cloudy interphase. The clear, aqueous phase was then transferred to an RNase-free tube. Then 0.7-0.8 volumes of isopropanol were

added. The tube was then mixed through vortexing and shaking the tube. The tube was then left to precipitate overnight at -20˚C.

About twenty-four hours later the tube was spun at 14,000 rpm for 30 minutes at 4˚C. As a result, there was then a barely visible pellet under the isopropanol and stuck to the side of the tube. The supernatant was then removed by pipet. The pellet was then washed with 500 µl of 75% ethanol which resulted in a visible pellet. The pellet was then spun at 14,000 rpm for 10 minutes. The supernatant was then removed again by pipet. The picofuge was then used to collect the remaining ethanol at the bottom of the tube and then removed the remaining supernatant by pipet. Once all of the other liquid was removed, the pellet was then redissolved in 10 µl RNase-free water. A NanoDrop™ spectrometer was then used to analyze the sample and to determine if the RNA isolation was a success. To use the program 1 µl of water was tested as a blank. After cleaning the stand, 1 µl of the RNA was tested on the stand. The resulting tube was then stored in a freezer at -80˚C.

cDNA Synthesis

For each reaction 1 µl RNA was combined with 1 µl of 10 mM dNTP mix, 1 µl 0.5 µg/µl oligo [dT] primer mix, and 7 µl DEPC-treated water. The RNA and primer mixture was then incubated at 65˚C for five minutes and then placed on ice

for one minute. Another master mix was then created with 2 µl 10X RT buffer, 4 µl 25mM $MgCl_2$, 2 µl 0.1 M DTT, and 1 µl of RNaseOUT (40 U/µl) for each of the two reactions run. Then 9 µl of the above master mix was added to each RNA and primer mixture.

The tubes were mixed and centrifuged. The tubes were then incubated at 42˚C for two minutes. Then 1 µl of SuperScript™ II RT reverse transcriptase was added to one of the tubes. The other tube served as the minus RT control and instead 1 µl of DEPC-treated water was added instead of the RT. The tubes were then incubated at 42˚C for fifty minutes and then the reaction was terminated at 70˚C for fifteen minutes. Then the tubes were chilled on ice. The reaction was exposed to a brief centrifugation to collect the reaction. Then 1 µl of RNase H was added to each tube, and the tubes were incubated for twenty minutes at 37˚C. The resulting reaction was stored at -20˚C.

Primer Design

The primers were selected for *dLipin* and *Actin 5c*. Ten primer sets were designed using the NCBI database primer tool, and three of those sets were then ordered from Integrated DNA technologies. The primers ordered contained both a forward and reverse sequence. From testing the primers through a gel

electrophoresis, this experiment used *dLipin* primer set two. *Actin 5c* primers were also used as a control.

Table 1. **Primers designed for *dLipin.***

Gene	Primer ID	Sequence
dLipin (set 1)	Forward	5’- AGC AGA GGG ACA ACA ACA GG- 3’
dLipin (set 1)	Reverse	5’- GCC GTA CGA CTA GGT TAG GC- 3’
dLipin (set 2)	Forward	5’- GCA GAG GGA CAA CAA CAG GT- 3’
dLipin (set 2)	Reverse	5’- ATG CAG CCA TCC AGG TGT AG- 3’
dLipin (set 3)	Forward	5’- AAG CAG CAG AGG GAC AAC AA- 3’
dLipin (set 3)	Reverse	5’- AAA TGC TGG GGC TTT TGC AC- 3’

PCR

A PCR must be performed to amplify a specific gene sequence through heating and cooling samples. In this case, the forward and reverse for the lipin primer set 2 (experimental gene of interest) and *Actin 5c* (housekeeping gene) were used. A master mix was prepared with 5.0 µl of 10X PCR buffer (minus $MgCl_2$), 6.0 µl 20 mM $MgCl_2$, 1.0 µl 10 mM dNTPs, 31.6 µl of nuclease-free water, and 0.4 µl of *Taq* polymerase 0.4 µl for each of the two reactions. In addition, 2.0 µl of 10 µM forward primer, 2.0 µl of 10 µM reverse primer, and 2.0 µl of cDNA were added for the corresponding *Actin 5c* and lipin tubes. The resulting master mix was split into four separate tubes, one with plus RT and lipin, one with plus RT and *Actin 5c*, one with minus RT and lipin, and a fourth with minus RT and *Actin 5c*. After all of the reagents were added into their Eppendorf tubes, they were then inserted into the thermocycler following the methods of the below table.

Table 2. Thermocycler profile for *dLipin* and *Actin 5c* RT-PCR amplification.

Stage	Temperature	Duration	Cycle Count
Denaturation	94˚C	30 sec	35 cycles
Annealing	58.2˚C	30 sec	
Extension	72˚C	30 sec	
Final Extension	72˚C	5 min	1
Final Hold	4˚C	Up to ∞	N/A

After the PCR was completed, the products were then ready for a gel electrophoresis that was used to visualize the PCR products. This tested if the cDNA was good and if the primers worked.

Gel electrophoresis

To run gel electrophoresis, 50 mL of 1x TAE was measured out into a small beaker and 0.8 g of agarose added to the TAE and mixed. The combined TAE and agarose was then microwaved until it boiled and then was removed and

swirled. This process was repeated until the agarose was mixed in and the solution was clear. Then 5 µl of Gel Red DNA Stain was added to the agarose and TAE mix and swirled. This mixture was poured into a gel mold and a comb was added to create the wells. The gel was then allowed to harden for ten to fifteen minutes when the gel became visibly cloudy. The gel was then removed and rotated so the wells were by the negative electrode. 1x TAE was then poured into the mold until the gel was submerged. The comb was then removed leaving wells. In the first well 10 µl of DNA ladder was added as a control. For each of the samples run, 2 µl of Gel Loading Buffer was added to each PCR tube and mixed. Then 20 µl of each sample was taken from the PCR tubes and loaded into the appropriate wells with notes taken on what was in each well. A lid was then placed on the gel and connected to a power supply and the charge set to 116 volts for twenty to thirty minutes. The gel was then allowed to run until the ladder was separated. After the gel was run, the power was disconnected, and an image was taken of the gel. Initial images taken came out with a blue tint and were edited later to remove the blue tint and turn the images into black and white.

Quantitative Real Time PCR (qPCR)

This study used relative quantification to complete a comparison between the target gene *dLipin* and the control gene, *Actin 5c*. The aim was to quantify the

dLipin expression in the *cg-Gal4; UAS-EcR-DN* fat bodies versus the wild-type fat bodies at the 0, 6, and 12 hour experimental time points.

Experimental qPCR Set Up

A total of 46 experimental wells were set up with 36 used to gather experimental data and 10 set up to generate standard curve data. The first qPCR run included only 36 experimental wells and excluded the wells for the standard curve data. Six experimental qPCR wells were set up for each experimental sample type: 2 wells containing cDNA with *dLipin* primers and one *dLipin* with no RT control; 2 wells containing cDNA with *Actin 5c* primers, and one *Actin 5c* no RT control. There was a total of 6 unique experiment sample types, wild type and *cg-Gal4; UAS-EcR-DN* fat body collected at 0, 6, and 12 hours APF. Each experiment contained 47.5 μl of the appropriate qPCR master mix and 2.5 μl of the appropriate cDNA. The qPCR was then run through the following thermocycler profile.

Table 3. Reaction Mixture for qPCR Reactions

Reagent	Amount Needed for 1 Reaction
BimakeTM SYBR Green Master Mix	25 µl
10 µM forward primer	2.5 µl
10 µM reverse primer	2.5 µl
ROX Reference Dye 2	1 µl
Nuclease-Free Water	16.5

Table 4. Thermocycler Profile Used in qPCR Reactions

Stage	Temperature	Time	Cycle Count
Hot Start	95 C	5 minutes	1
Amplification	95 C	15 seconds	40
	60 C	1 minute	
Melt	95 C	30 seconds	1
	65 C	30 seconds	
	95 C	30 seconds	

qPCR Standard Curves and Primer Efficiencies

The Pfaffl method for qPCR analysis was used to analyze the resulting qPCR data. The method requires controls in each model to standardize the reaction (Pfaffl, 2001). To do this, whole body cDNA was synthesized from 4-5, 0 hr APF wild-type pupae. The whole body cDNA was diluted into serial dilutions, starting with undiluted cDNA, and adding nuclease-free water in the successive dilutions. The dilutions began with a 1/1 (undiluted) cDNA and adding 10 µl of this to 10 µl of nuclease free water to achieve a 1/2 cDNA dilution, adding 10µl of the 1/2 cDNA to 10 µl of nuclease free water to achieve a 1/4 cDNA dilution, adding 10 µl of the 1/4 cDNA to 10 µl of nuclease free water to achieve a 1/8 dilution, and adding 10 µl of the 1/8 dilution to 10 µl of nuclease free water to achieve a 1/16 dilution. These serial dilutions were then used in the qPCR to set standard amplification curves for the *dLipin* and *Actin 5c* primer efficiencies. The serial dilutions used 10 experimental qPCR wells with 5 for *dLipin* and 5 for *Actin 5c* using the 1/1, 1/2, 1/4, 1/8, and 1/16 dilutions created.

After the qPCR reactions, Ct values from the standard curve wells were plotted as Y values against the X values of each cDNA concentration. The slope of the concentration vs the Ct value lines was used to determine the primer amplification efficiencies using equation 1.

$$Efficiency = 10^{\left(-\frac{1}{slope}\right)}$$

(Equation 1 (Pfaffl, 2001))

qPCR Data Analysis

The qPCR data was analyzed using the Pfaffl method as outlined in Pfaffl (2001). The model aims to determine the quantification or expression of a target gene in comparison to a reference gene. The equation takes into account the primer efficiency. This experiment used *Actin 5c* as a reference gene and *dLipin* as the target gene. The equation developed uses the efficiency of the target gene transcript and the efficiency of a reference gene transcript (Pfaffl, 2001). The values needed for this experiment include the control and experimental values for genes being tested and the control and experimental values for the reference gene. The results are expressed as a ratio of the change in Cq values between *dLipin* amplification in w^{1118} fat body and *cg-Gal4; UAS-EcR-DN* fat body compared to the *Actin 5c* delta Cq values between *Actin 5c* amplification in w^{1118} fat body and *cg-Gal4; UAS-EcR-DN* fat body while also considering qPCR primer amplification efficiencies (Equation 2). This ratio was found for each of the experimental time points. The Pfaffl equation refers to CP values instead of Cq values; the two are interchangeable.

$$\text{ratio} = \frac{(E_{\text{target}})^{\Delta \text{CP}_{\text{target}}(control - sample)}}{(E_{\text{ref}})^{\Delta \text{CP}_{\text{ref}}(control - sample)}}$$

(Equation 2 (Pfaffl, 2001))

RESULTS

Visualization of PCR Products via Gel Electrophoresis

Gel electrophoresis was used to visualize the PCR products and to determine the success of the PCR primers and cDNA synthesis. Successful PCR was achieved at all of the experimental time points from both the w^{1118} fat body and the *cg-Gal4; UAS-EcR-DN* fat body. PCR amplification was visible at the 0, 6, and 12 hour time points. This was seen through successful amplification of both *Actin 5c* and *dLipin*. For both the w^{1118} and *cg-Gal4; UAS-EcR-DN* at each of the time points there were bright bands that showed up for the *Actin 5c* and *dLipin* amplification.

PCR amplification was successful for the 12 hour amplification of the w^{1118} and *cg-Gal4; UAS-EcR-DN* samples. w^{1118} samples provided clear bands for both *Actin 5c* and *dLipin* in their respective lanes (See figure 4). Primer dimer is visible in all of the lanes and there is a thin band in the *Actin 5c* -RT lane. The *cg-Gal4; UAS-EcR-DN* samples produced clear bands for both *Actin 5c* and *dLipin* (see figure 5). Primer dimer is also visible in each of the loaded lanes.

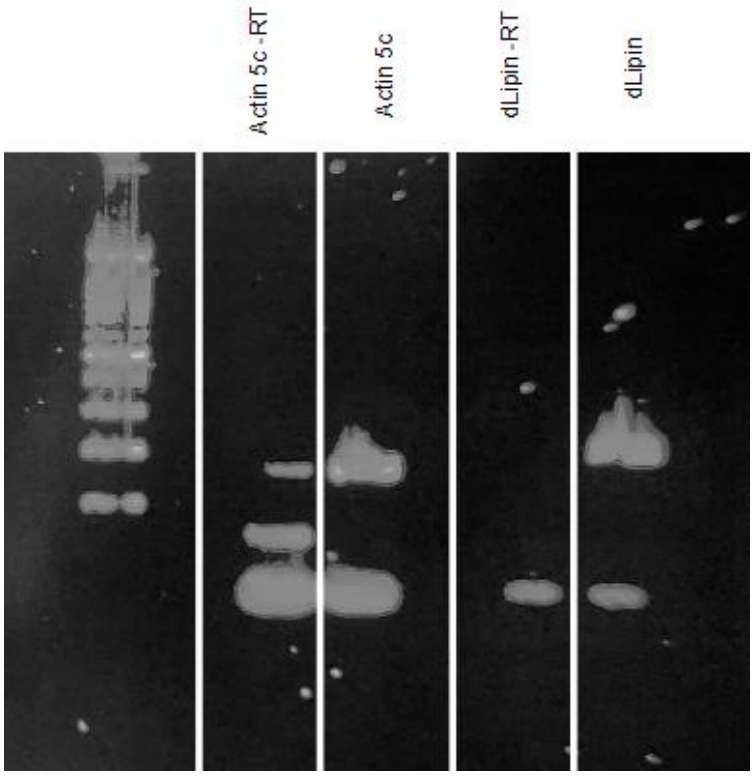

Figure 4. Image of the gel electrophoresis run on PCR products of cDNA synthesized from RNA of *w*^{1118} dissected from prepupa aged 12 hours APF. This image clearly demonstrates successful PCR amplification of both *Actin 5c* and *dLipin*.

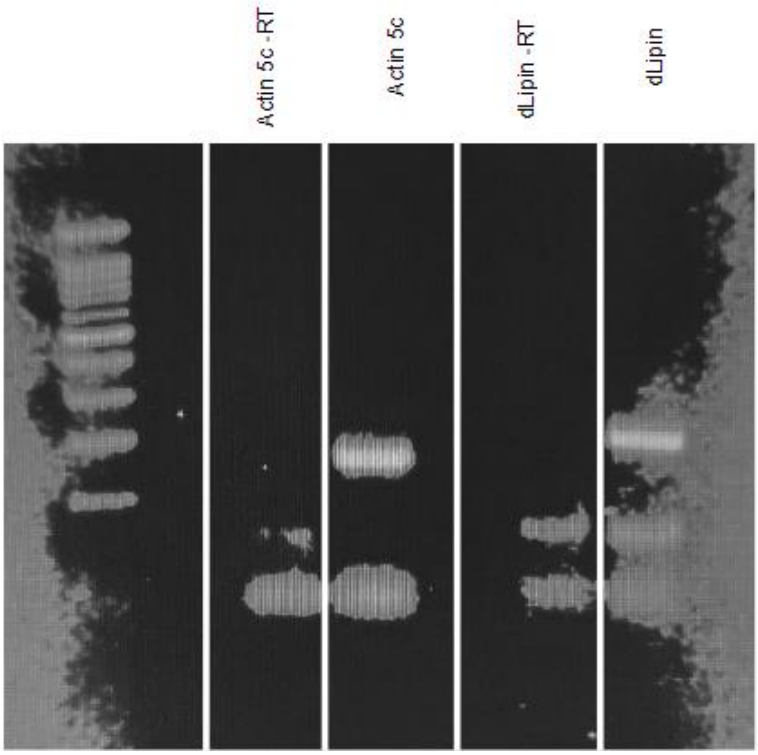

Figure 5. Image of the gel electrophoresis run on PCR products of cDNA synthesized from RNA of *cg-Gal4; UAS-EcR-DN* dissected from prepupa aged 12 hours APF. This image clearly demonstrates successful PCR amplification of both *Actin 5c* and *dLipin.*

PCR amplification was successful for the 6 hour amplification of the w^{1118} and *cg-Gal4; UAS-EcR-DN* samples. w^{1118} samples provided clear bands for both *Actin 5c* and *dLipin* in their respective lanes (See figure 6). Primer dimer is visible in each of the -RT lanes and is less visible in the *Actin 5c* and *dLipin* lanes but still present. There is a thin band visible in the *Actin 5c* -RT lane. The *cg-Gal4;*

UAS-EcR-DN samples also produced clear bands for both *Actin 5c* and *dLipin* (see figure 7). Primer dimer is also visible in each of the loaded lanes.

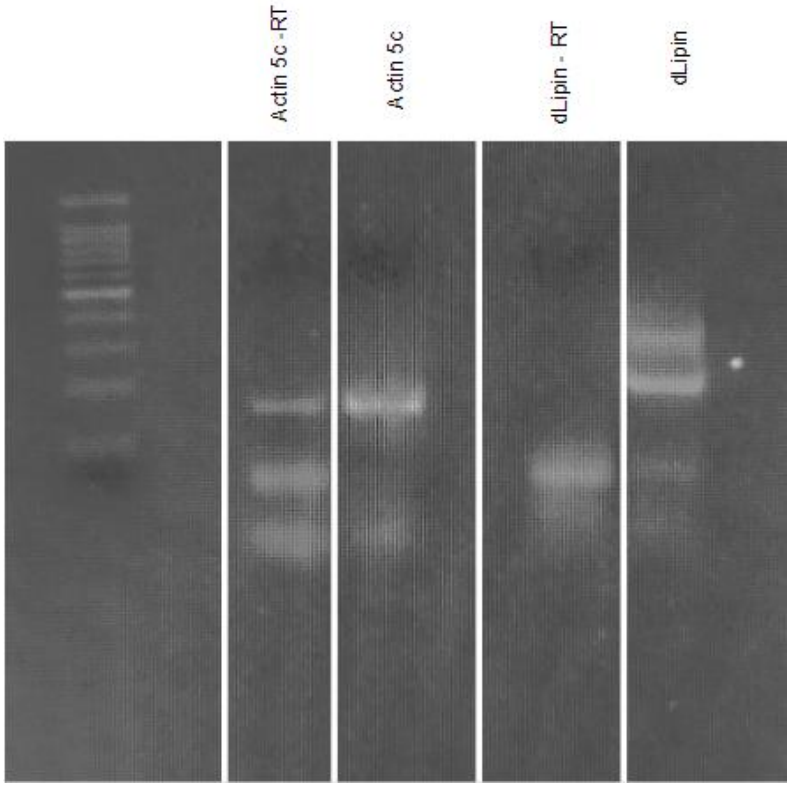

Figure 6. Image of the gel electrophoresis run on PCR products of cDNA synthesized from RNA of w^{1118} dissected from prepupa aged 6 hours APF. This image clearly demonstrates successful PCR amplification of both *Actin 5c* and *dLipin*.

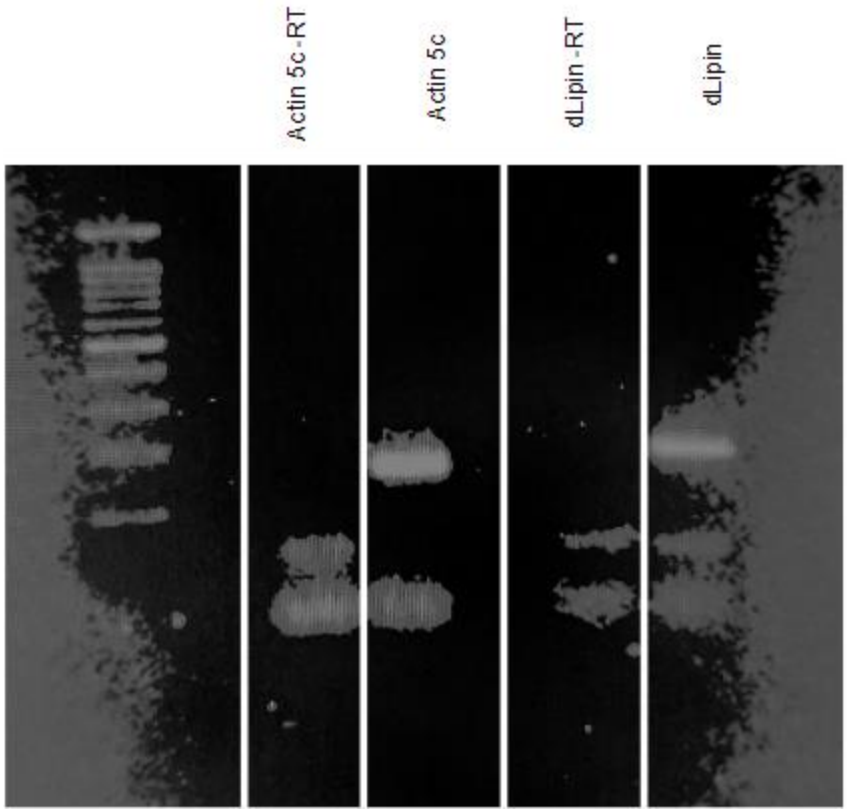

Figure 7. Image of gel electrophoresis run on PCR products of cDNA synthesized from RNA of *cg-Gal4; UAS-EcR-DN* dissected from prepupa aged 6 hours APF. This image clearly demonstrates successful PCR amplification of both *Actin 5c* and *dLipin*.

PCR amplification was successful for the 0 hour amplification of the w^{1118} and *cg-Gal4; UAS-EcR-DN* samples. w^{1118} samples provided clear bands for both *Actin 5c* and *dLipin* in their respective lanes (See figure 8). Primer dimer is visible in each of the loaded lanes. There are bands visible for the -RT lanes for both *Actin 5c* and *dLipin*, though the *dLipin* -RT band is much thinner and fainter. *The*

cg-Gal4; UAS-EcR-DN samples also produced clear bands for both *Actin 5c* and *dLipin* (see figure 9). Primer dimer bands are present in the loaded lanes, but the primer dimer is more visible in the -RT lanes and fainter in the *Actin 5c* and *dLipin* lanes.

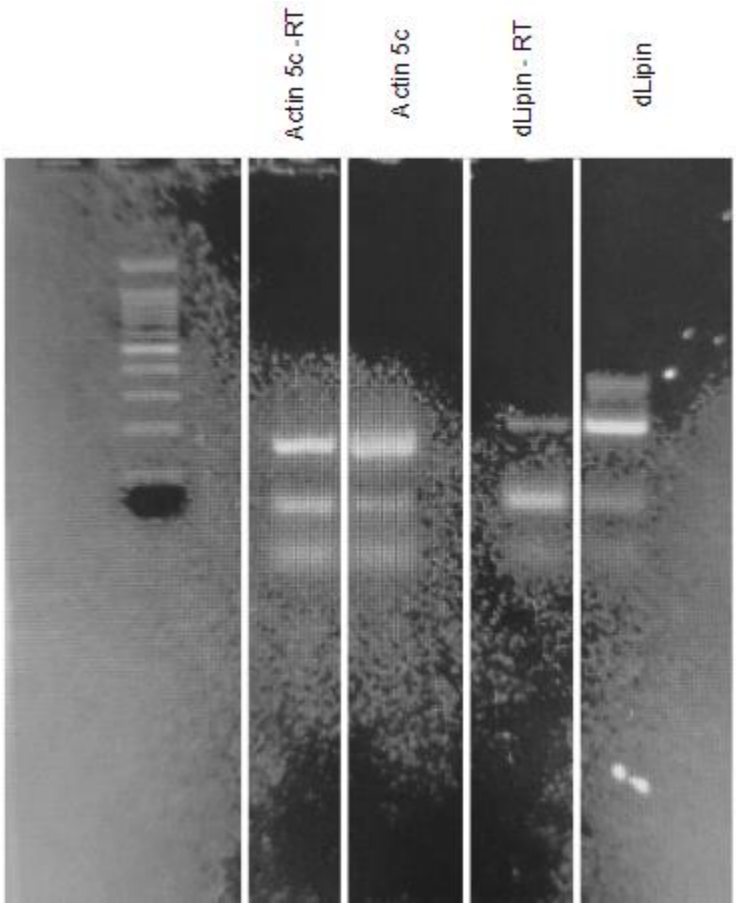

Figure 8. Image of gel electrophoresis run on PCR products of cDNA synthesized from RNA of w^{1118} dissected from prepupa at 0 hours APF. This image clearly demonstrates successful PCR amplification of *Actin 5c* and *dLipin*.

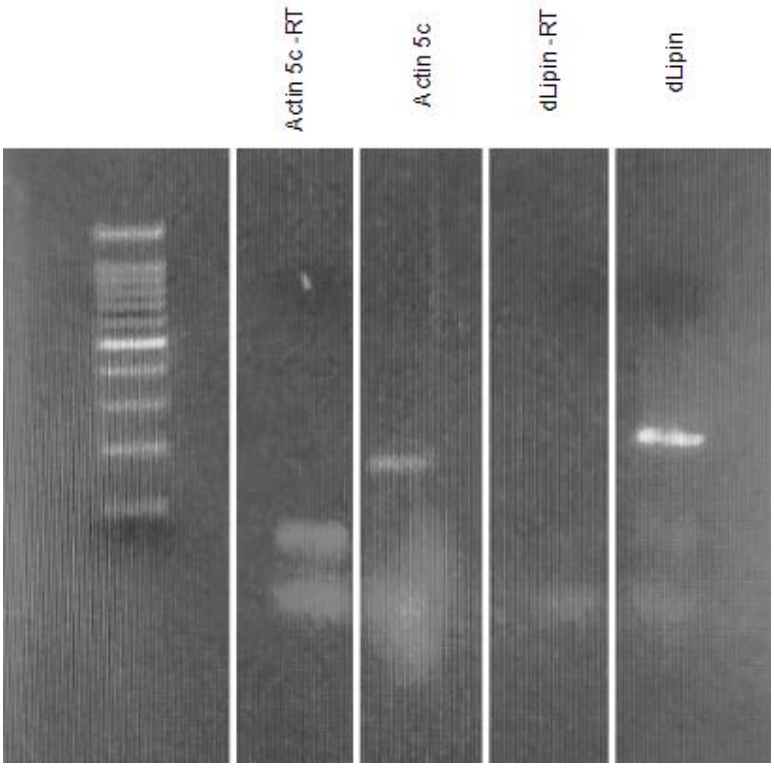

Figure 9. Image of the gel electrophoresis run on PCR products of cDNA synthesized from RNA of *cg-Gal4; UAS-EcR-DN* dissected from prepupa at 0 hours APF. This image clearly demonstrates successful PCR amplification of both *Actin 5c* and *dLipin*.

Primer Efficiencies

To correct for primer efficiencies, the Pfaffl method uses standard curves on each qPCR plate. Standard curves were generated for both *Actin 5c* and *dLipin* using serial dilutions of cDNA synthesized from w^{1118} whole body animals at 0

hours APF. The standard curve was not included on my first plate but was included on my second plate for qPCR. The standard curve is placed on the experimental plate to determine the amplification efficiency of the particular qPCR.

Prior to running a qPCR plate, I ran a plate that was just a standard curve to check primer efficiency. For the initial plate the 1/1, 1/2, 1/4, 1/8, and 1/16 dilutions were generated for the *Actin 5c* primer standard curve. The resulting standard curve slope for *Actin 5c* was -17.77 (see figure 10). This was more negative than expected, this is likely due to an excess of primer dimer in the solution. From this slope, the efficiency of the *Actin 5c* primer was calculated as 1.138 using equation 1.

The *dLipin* standard curve used the 1/1, 1/4, 1/8, and 1/16 dilutions. The 1/2 dilution didn't yield any Cq value and was removed from the analysis. The standard curve slope for dLipin was -3.13 (see figure 11). From this slope, the efficiency of the *dLipin* primer was calculated as 2.086 using equation 1.

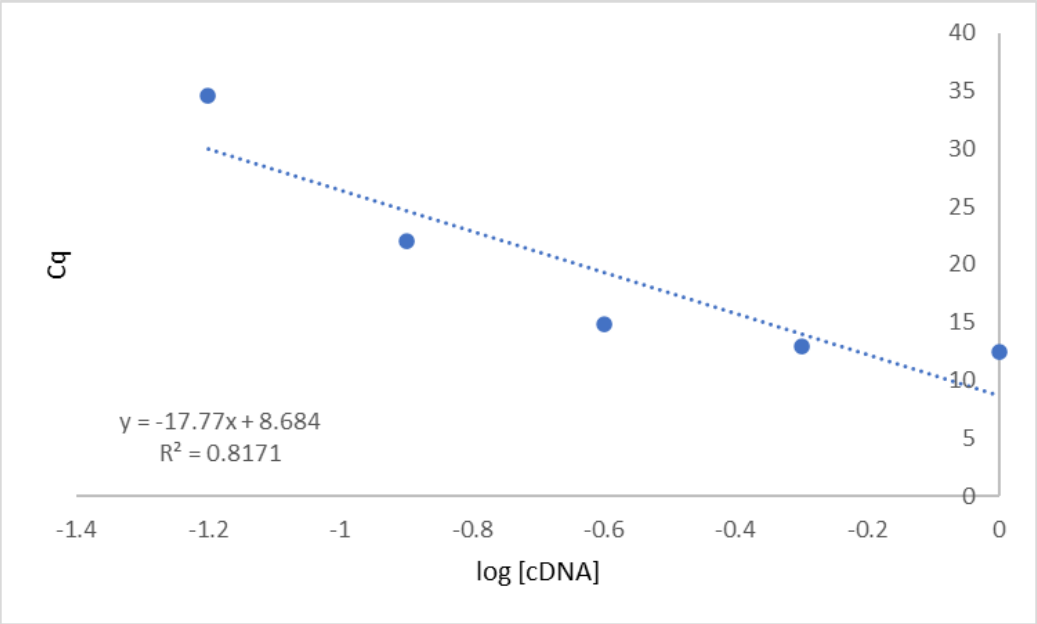

Figure 10. *Actin 5c* primer standard curve. The log of serial diluted cDNA from whole body w^{1118} *Drosophila* at 0 hours APF. The slope of the standard curve was used to determine the *Actin 5c* primer amplification efficiency. The slope of -17.77 yielded an efficiency of 1.138.

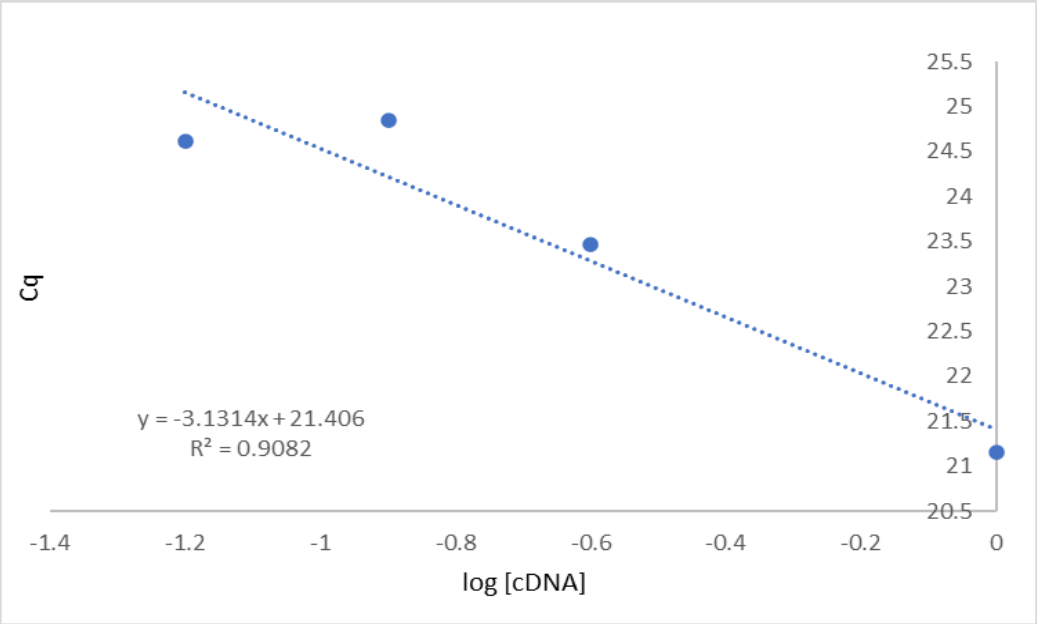

Figure 11. *dLipin* primer standard curve. The log of serial diluted cDNA from whole body w^{1118} *Drosophila* at 0 hours APF plotted against DNA concentration in each serial dilution. The slope of the standard curve was used to determine the *dLipin* primer amplification efficiency. The slope of -3.1314 yielded an efficiency of 2.086.

The second qPCR plate run included standard curves for *Actin 5c* and *dLipin* to check primer efficiency. For this plate the 1/1, 1/2, 1/4, 1/8, 1/16 dilutions were generated for the *Actin 5c* primer standard curve. The resulting standard curve slope for *Actin 5c* was -4.5867 (see figure 12). This value is higher than ideal but close to the ideal. From this slope, the efficiency of the *Actin 5c* primer was calculated as 1.65 using equation 1.

The *dLipin* standard curve also used the 1/1, 1/2, 1/4, 1/8, and 1/16 dilutions. The resulting standard curve slope for dLipin was -4.1233 (see figure 13). The slope was similar to the slope for *Actin 5c* and is higher than ideal but close enough to be considered efficient. From this slope, the efficiency of the *dLipin* primer was calculated as 1.748 using equation 1.

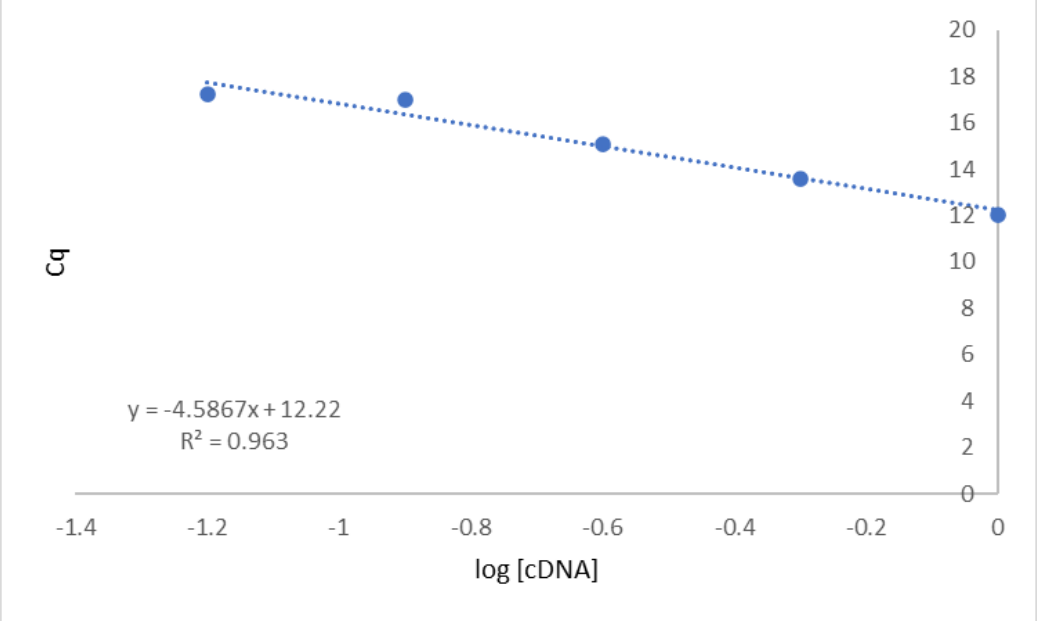

Figure 12. *Actin 5c* primer standard curve. The log of a serial diluted cDNA from whole body w^{1118} *Drosophila* at 0 hours APF plotted against the DNA concentration in each serial dilution. The slope of this standard curve was used to determine the *Actin 5c* primer amplification efficiency. The slope of -4.5867 yielded an efficiency of 1.65.

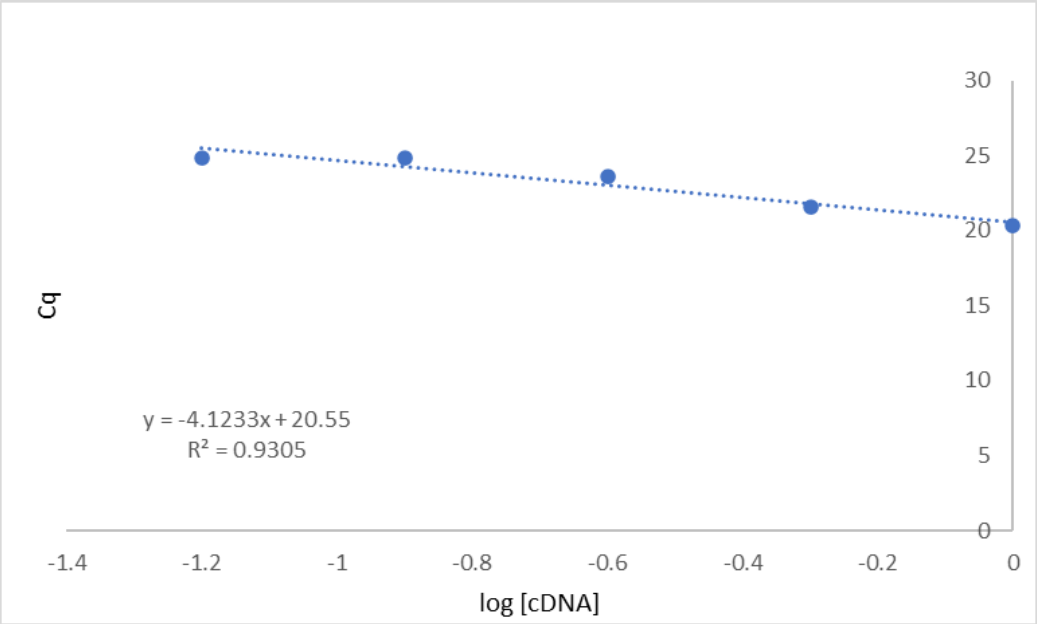

Figure 13. *dLipin* primer standard curve. The log of the serial diluted cDNA from whole body w^{1118} *Drosophila* at 0 hours APF plotted against DNA concentrated in each serial dilution. The slope of the standard curve was used to determine the *dLipin* primer amplification efficiency. The slope of -4.1233 yielded an efficiency of 1.748.

Quantitative Real-Time PCR Standard Curves and Primer Efficiencies

The hypothesis for this experiment predicted a downregulation of *dLipin* in the *cg-Gal4; UAS-EcR-DN* fat bodies at 0, 6, and 12 hours APF. Results from the qPCR ran counter to the hypothesis. Normalized gene expression means the fold change in the wild-type expression ratio will always be one, according to the Pfaffl method. Expression ratios will indicate expression levels. If the ratio is larger than one, it indicates over-expression, while if the ratio is less than one it

will indicate under-expression. Only one of the two qPCR plates was run with a standard curve. The data below includes the data from the qPCR plate that included the standard curve and the averages from both of the plates using the standard curve efficiencies from the second plate. The values didn't differ that much between the two qPCR plates.

The following data is from the average of the two plates run. The expression ratio for 0 hours APF was 1.62 indicating overexpression of *dLipin* in the *cg-Gal4; UAS-EcR-DN* fat body compared to the w^{1118} fat body. The expression ratio for 6 hours APF was 2.5 indicating overexpression of *dLipin* in the *cg-Gal4; UAS-EcR-DN* fat body compared to the w^{1118} fat body. The expression ratio for 12 hours APF was 4.04 indicating overexpression of *dLipin* in the *cg-Gal4; UAS-EcR-DN* fat body compared to the w^{1118} fat body.

The following data is from the qPCR plate that was run that included a standard curve on the plate. The expression ratio for 0 hours APF was 1.91 indicating overexpression of *dLipin* in the *cg-Gal4; UAS-EcR-DN* fat body compared to the w^{1118} fat body. The expression ratio for 6 hours APF was 3.09 indicating overexpression of *dLipin* in the *cg-Gal4; UAS-EcR-DN* fat body compared to the w^{1118} fat body. The expression ratio for 12 hours APF was 12.19 indicating overexpression of *dLipin* in the *cg-Gal4; UAS-EcR-DN* fat body compared to the w^{1118} fat body.

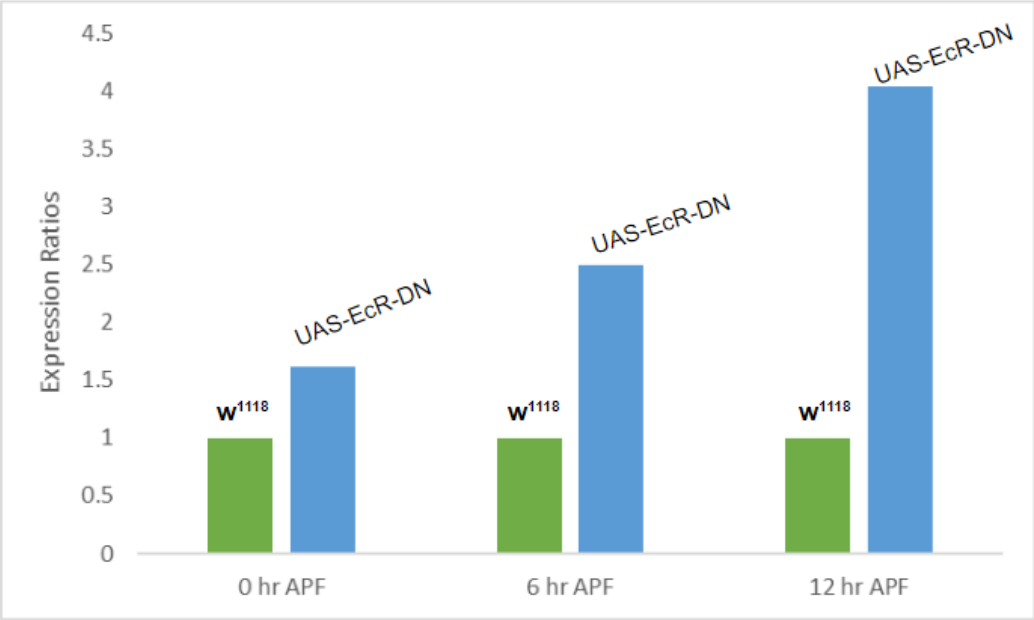

Figure 14. *dLipin* expression ratios from qPCR experiments using average of the two qPCR plates. Expression ratios of *dLipin* compared to *Actin 5c* expression in *cg-Gal4; UAS-EcR-DN* compared to w^{1118} fat body expressed. In comparison to wild-type expression represented as a ratio of one. At 0 hours APF, the expression ratio is greater than one, indicating an over-expression of *dLipin* in the larval fat body. At 6 hours APF, the expression ratio is greater than one, indicating an over-expression of *dLipin* in the larval fat body. At 12 hours APF, the expression ratio is greater than one, indicating an over-expression of *dLipin* in the larval fat body.

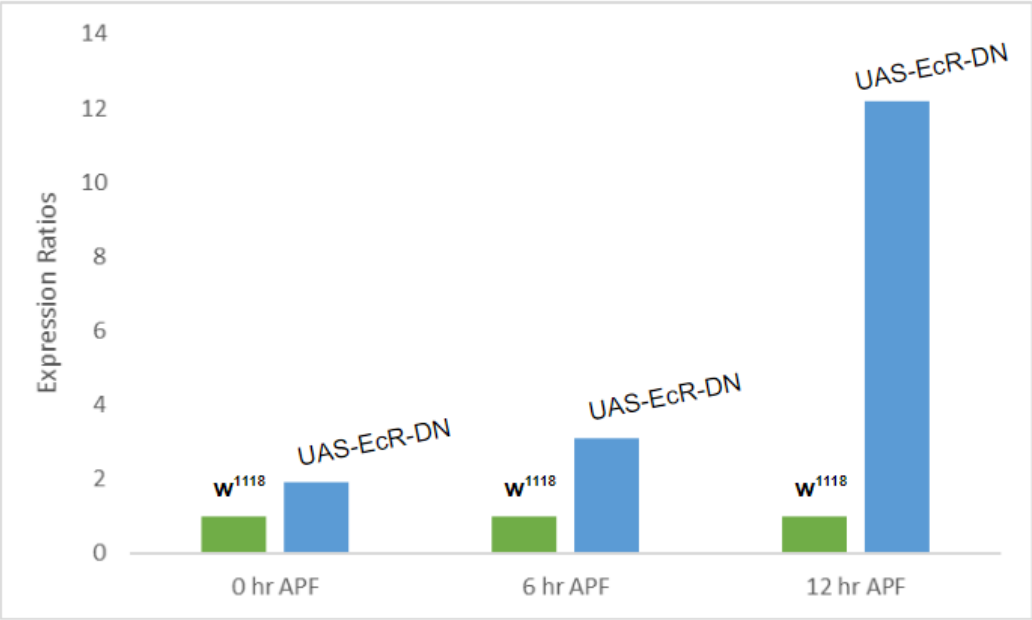

Figure 15. *dLipin* expression ratios from qPCR experiments using the qPCR plate with a standard curve. Expression ratios of *dLipin* compared to *Actin 5c* expression in *cg-Gal4; UAS-EcR-DN* compared to w^{1118} fat body expressed. In comparison to wild-type expression represented as a ratio of one. At 0 hours APF, the expression ratio is greater than one, indicating an over-expression of *dLipin* in the larval fat body. At 6 hours APF, the expression ratio is greater than one, indicating an over-expression of *dLipin* in the larval fat body. At 12 hours APF, the expression ratio is greater than one, indicating an over-expression of *dLipin* in the larval fat body.

The data was also calculated as log fold changes. The values came from taking the log of the expression ratios. If the results are positive, it would indicate over-expression and if they were negative, it would indicate under-expression. The figures demonstrate similar trends to the expression ratios with all of the values indicating over-expression at 0, 6, and 12 hours APF. The result of the average of the two qPCR plates depicts overexpression of *dLipin* in the *cg-Gal4;*

UAS-EcR-DN fat body as 0.21 at 0 hours APF, 0.398 at 6 hours APF and 0.606 at 12 hours APF. The result of the qPCR plate with the standard curve included, depicted overexpression of *dLipin* in the *cg-Gal4; UAS-EcR-DN* fat body as 0.281 at 0 hours APF, 0.49 at 6 hours APF, and 1.086 at 12 hours APF.

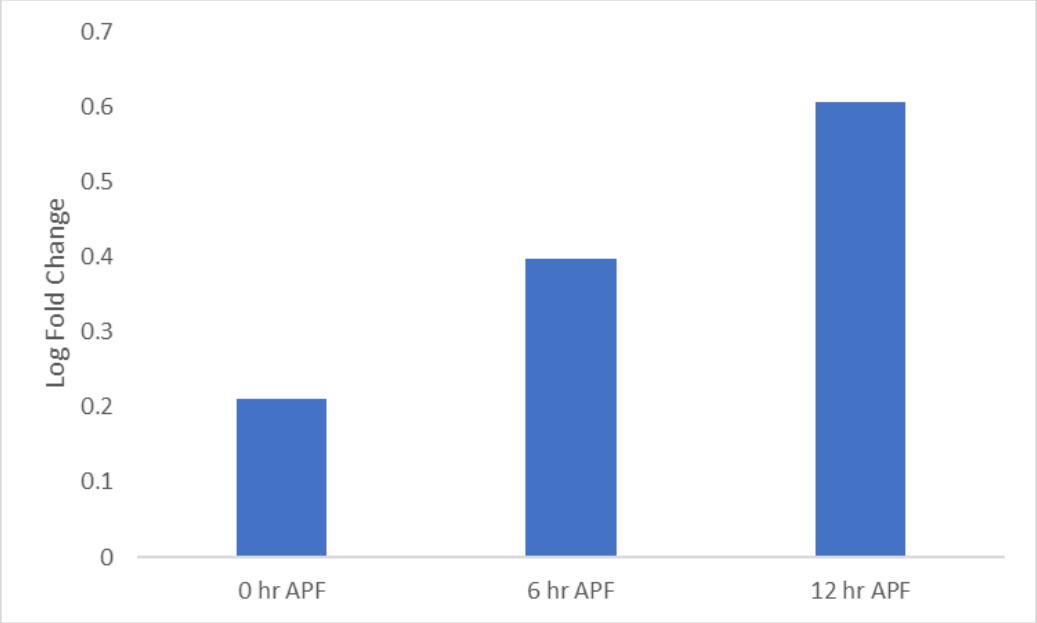

Figure 16. Log fold change of *dLipin* expression in *cg-Gal4; UAS-EcR-DN* fat body compared to w^{1118} fat body for the average of the two qPCR plates. Values were obtained by taking the log of the expression ratios. Zero represents wild-type expression, positive values indicate over-expression, and negative values indicate under-expression. The log fold change value of 0.21 at 0 hours APF indicates over-expression of *dLipin* in the larval fat body. The log fold change of 0.398 at 6 hours APF indicates over-expression of *dLipin* in the larval fat body. The log change of 0.606 at 12 hours APF indicates over-expression of *dLipin* in the larval fat body.

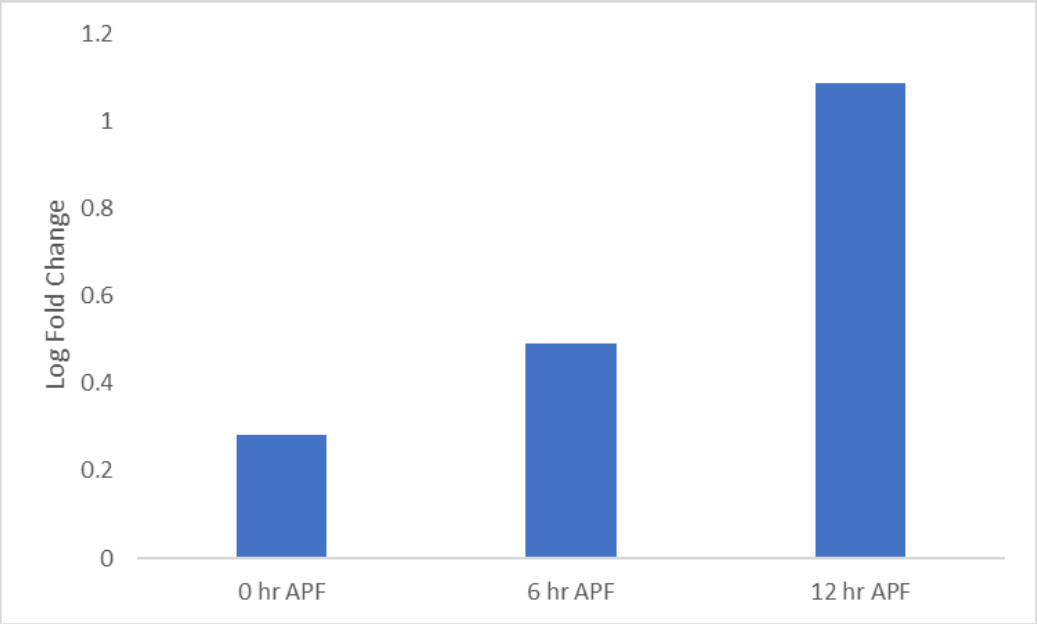

Figure 17. Log fold change of *dLipin* expression in *cg-Gal4; UAS-EcR-DN* fat body compared to w^{1118} fat body for the qPCR plate with the standard curve included. Values were obtained by taking the log of the expression ratios. Zero represents wild-type expression, positive values indicate over-expression, and negative values indicate under-expression. The log fold change value of 0.281 at 0 hours APF indicates over-expression of *dLipin* in the larval fat body. The log fold change of 0.49 at 6 hours APF indicates over-expression of *dLipin* in the larval fat body. The log change of 1.086 at 12 hours APF indicates over-expression of *dLipin* in the larval fat body.

DISCUSSION

PCR and Gel Electrophoresis

Results from the PCR and gel electrophoresis were successful. There were differences in primer dimer's presence. Imaging of the gel electrophoresis products differed slightly and may have led to alterations in primer dimer appearance and strength of the bands. Each gel demonstrated the presence of both *Actin 5c* and *dLipin* in all of the sample types. This also demonstrated successful cDNA synthesis and primer design. The resulting gel image for the 0 hour APF w^{1118} demonstrated the presence of *Actin 5c* and *dLipin*, however there was a band in the *Actin 5c* -RT lane that was equal to the band in the *Actin 5c* lane that wasn't the result of primer dimer. This indicates possible sample contamination in the *Actin 5c* -RT sample.

While successful gel images were obtained for each experimental condition, there were unsuccessful attempts previously. The primer pair used in this experiment was designed and was the second attempt at a successful primer pair. The initial primer pair tested yielded no visible band for *dLipin*. Fortunately, the second primer pair designed and tested was successful and yielded a visible band for *dLipin*. Prior to these final images, there were several gels run that resulted in only primer dimer being visible when imaged. This was likely due to a mistake made during cDNA synthesis or PCR. There are also differences in clarity of the gel images as we received a new imager that I struggled in using

resulting in the differences. The differences make it more difficult to compare band brightness levels between the different gels.

Potential Experimental Error: PCR and gel electrophoresis

Gel imaging result success was mixed prior to the end results and gel images presented above. This was likely due to a mistake in the process that led to unsuccessful PCR amplification that was later corrected to provide the resulting gels. The imager was also new and led to complications in imaging that resulted in my being unable to determine the brightness of the bands. The differing brightness and quality of the images also makes it difficult to fully determine what is occurring visually. It may have been beneficial to develop imaging protocol to make sure the images all had the same clarity and could be compared to each other in a better and clearer way.

RNA Concentrations

RNA concentrations were measured for each sample after the RNA was isolated and prior to cDNA synthesis. All of the samples had a concentration well above 200 ng/µl. The samples also had 260/280 values that were close to 2.0 with the highest value at 2.16 and the lowest at 1.91. These values indicate that the RNA was well isolated and likely not very contaminated with other things such as

proteins or a reagent used in the reaction. The values were close in number between the w^{1118} and the *cg-Gal4; UAS-EcR-DN* genotypes. The *cg-Gal4; UAS-EcR-DN* genotype resulted in 260/280 values of 2.07 for 0 hours APF, 2.1 for 6 hours APF, and 2.1 for 12 hours APF. The w^{1118} genotype resulted in 260/280 values of 2.1 for 0 hours APF, 2.16 for 6 hours APF, and 1.91 for 12 hours APF. There was more variation in the w^{1118} genotype's ratios than the *cg-Gal4; UAS-EcR-DN* genotype's ratios.

cDNA Synthesis

Initial issues in unsuccessful gel electrophoresis images were likely due to issues in cDNA synthesis. After a few failed gel electrophoresis images, the PCR was rerun and resulted in another unsuccessful gel image. This indicates that it was not an issue with the PCR but rather with the cDNA synthesis process. When cDNA synthesis was rerun using the same RNA that had been isolated, and then PCR was run it resulted in successful gel electrophoresis images. PCR primers were kept consistent throughout the study while the cDNA varied which indicated lack of successful amplification was due to cDNA rather than primer design.

Primers

While in the end, the PCR amplification and gel electrophoresis resulted in success, there may have been potential errors in the *dLipin* primer. For this experiment, I designed my own primer pair to use. Given the lack of literature on *dLipin* in general, there was no recommended primer pair to use. The first primer pair test failed to produce any bands in the *dLipin* lane. The second primer pair on the other hand did result in a successful band in the *dLipin* lane. The standard curves produced for *dLipin* did show that the primer pair was efficient. Still, it may have been beneficial to test the efficiencies for multiple different primer pairs for *dLipin*. Especially since there is a lack of literature on the primer pair to use and there were ten options in the NCBI database primer tool.

Quantitative PCR Results

qPCR results were opposite of what was expected at each of the experimental time points. The qPCR results demonstrated an unexpected upregulation of *dLipin* in each of the time points. The upregulation also increased at 0, 6, and 12 hours APF. There was an observed up-regulation at 0 hours APF seen in both an expression ratio higher than one and a positive log-fold change for qPCR results from both the average of the two plates and the plate that included the standard curve. There was also an observed up-regulation at 6 hours APF seen

in both an expression ratio higher than one and a positive log-fold change for qPCR results from both the average of the two plates and the plate that included the standard curve. The up-regulation at 6 hours APF was higher than it was at 0 hours APF. There was also an observed up-regulation at 12 hours APF seen in both an expression ratio higher than one and a positive log-fold change for qPCR results from both the average of the two plates and the plate that included the standard curve. The up-regulation at 12 hours APF was higher than it was at 0 hours APF and 6 hours APF.

The upregulation of *dLipin* at each of the experimental time points indicates that in the *cg-Gal4; UAS-EcR-DN* fat bodies in comparison to the w^{1118} fat bodies indicates that ecdysone signaling instead inhibits *dLipin* transcription. This is based on the high expression ratios and log-fold change values from this experiment. These results came from the *cg-Gal4; UAS-EcR-DN* fat bodies where ecdysone was inhibited. In the w^{1118} fat bodies, ecdysone is not inhibited. If my hypothesis were true and ecdysone signaling activated the transcription of the *dLipin* gene, then the results would have shown down-regulation in the *cg-Gal4; UAS-EcR-DN* fat bodies with expression ratios under one and negative log-fold change values. Instead, the opposite was shown and inhibition of ecdysone signaling appears to inhibit transcription of the *dLipin* gene.

Possible Experimental Error: qPCR

qPCR reactions were carried out twice during this experiment. Only one of the plates included a standard curve on the plate while the other didn't. For both of the qPCR plates, the samples were only run in duplicate with a -RT control attached. The samples were only run in duplicate due to a cDNA limitation. It would have been beneficial to run plates that had the samples in triplicate to further confirm the results provided. The qPCR plates run appeared to be generally successful, all of the amplification curves followed the same normal curve shape. Given one of the plates was run without wells dedicated to a standard curve, there is a possibility that the data could be less reliable. The initial standard curve test plate run showed an abnormally high efficiency for Actin 5c indicating that primer dimer was present and affected the standard curve results.

Conclusions

In conclusion, results from qPCR experiments run counter to the hypothesis that ecdysone signaling activates the transcription of the *dLipin* and instead indicates that ecdysone inhibits the transcription of the *dLipin* gene at 0, 6, and 12 hours APF. Even with the possible locations for experimental error in this experiment, there is a possibility that the results found in this study are true.

Despite my prior understanding of the relationship between *dLipin* and ecdysone, I have a few theories as to why the data turned out opposite of what was expected. A key role of ecdysone in metamorphosis is inducing apoptosis of larval cells to destroy larval cells and replace them with adult tissues. In *dLipin* loss-of-function studies they have found that nuclear fragmentation occurs that looks very similar to apoptosis (Ugrankar *et al*., 2011). There is a possibility that ecdysone downregulates *dLipin* to assist in apoptosis to destroy larval cells and replace them. During metamorphosis, ecdysone signaling may down-regulate *dLipin* to cause something similar to loss-of-function in *dLipin* that leads to nuclear fragmentation and altered mitochondria that indicate the cell must undergo and potential assists in the programed cell death experienced during *Drosophila* metamorphosis. The death of these larval cells allows for the limited nutrients available during metamorphosis to be taken up by the new, adult cells. The older cells' destruction also allows for their nutrients to be metabolized by the newer cells. The larval cells during metamorphosis provide a potential energy source for the newer cells. So, a possible explanation for the down-regulation of *dLipin* during metamorphosis is to allow for the cells to destruct in a form similar to apoptosis so the nutrients produced can be taken up by younger, adult cells created for adult structures. Further research on the relationship between *dLipin* and the apoptotic pathway may illuminate the potential connection between the two during metamorphosis.

dLipin's role under starvation conditions may also provide an explanation for these results. *dLipin* was found to have a role in immune response genes and the genomic effects of certain nutrients (Hood *et al*., 2020), it could be possible that *dLipin* could block the ability of certain nutrients used. Since metamorphosis is a period without feeding, all nutrients are needed to survive metamorphosis and if *dLipin* blocks some of the nutrients it could be downregulated to make all nutrients available. Research on *dLipin* is not specific on what the gene's role is in immune response genes and how it regulates certain nutrients. There is a possibility that *dLipin* in its response to starvation conditions may regulate the use of certain nutrients more than others. Given how energetically expensive metamorphosis is and how long the process is, it may not be as beneficial to hold back certain nutrients. In order to undergo metamorphosis, the *Drosophila* must reach a critical weight which indicates the particular level of nutrient stores are crucial to metamorphosis. This critical weight must be within reason as the *Drosophila* larva won't always have access to excess nutrients. The down-regulation of *dLipin* by ecdysone may allow for the larva to make the most of the nutrients it has stored. The study done by Hood *et al*. (2020) was done in *Drosophila* adults and may not apply in the same way to *Drosophila* larva. To my knowledge, there has been no study conducted on if *dLipin* is up-regulated or down-regulated during *Drosophila* larval stages and this may further assist in understanding the relationship between *dLipin* and ecdysone.

Future Directions

Future research should involve re-running qPCR using cDNA that has shown successful gel images. Since the qPCR was only run in duplicate, it would be beneficial to confirm the results through additional testing. This would further help in confirming the results found during this experiment or disprove these experiment results. This would be beneficial in determining other followup experiments given that the end results were opposite of my original hypothesis and understanding of *dLipin* and ecdysones relationship.

It may also be helpful to run western blots. The qPCR run has provided data on the relative expression levels of *dLipin*. A western blot would be able to provide more information such as what the protein level of *dLipin* may be. Having data on both qPCR and a western blot would provide insight into how the gene is regulated as the mRNA level provided by the qPCR may not be proportional to the protein level that would be provided by the western blot.

To answer the above potential explanations for the results of my experiment there are a few different studies that could be run. Different studies may include those looking into the relationship between *dLipin* and apoptosis and the apoptotic pathway. Additionally, it could be beneficial to look at *dLipin's* response to starvation conditions in larva. Studies have looked at *dLipin's* response to starvation conditions during adulthood, but there may be a difference between the adult and larval stages.

APPENDIX

Appendix 1- qPCR set up

1	2	3	4	5	6	7	8	9	10	11	12
Standard 1:1 Actin 5c	Standard 1:2 Actin 5c	Standard 1:4 Actin 5c	Standard 1:8 Actin 5c	Standard 1:16 Actin 5c	Blank	Blank	Blank	Blank	Blank	Blank	Blank
Standard 1:1 Lipin	Standard 1:2 Lipin	Standard 1:4 Lipin	Standard 1:8 Lipin	Standard 1:16 Lipin	Blank	Blank	Blank	Blank	Blank	Blank	Blank
w^{118} 0 hr Actin 5c RT	w^{118} 0 hr Actin 5c RT	w^{118} 0 hr Actin 5c RT	w^{118} 0 hr Actin 5c No RT	Blank	Blank	Blank	Blank	cg-Gal4;UAS-EcR-DN 0 hr Actin 5c RT	cg-Gal4;UAS-EcR-DN 0 hr Actin 5c RT	cg-Gal4;UAS-EcR-DN 0 hr Actin 5c RT	cg-Gal4;UAS-EcR-DN 0 hr Actin 5c No RT
w^{118} 0 hr dLipin RT	w^{118} 0 hr dLipin RT	w^{118} 0 hr dLipin RT	w^{118} 0 hr dLipin No RT	Blank	Blank	Blank	Blank	cg-Gal4;UAS-EcR-DN 0 hr dLipin RT	cg-Gal4;UAS-EcR-DN 0 hr dLipin RT	cg-Gal4;UAS-EcR-DN 0 hr dLipin RT	cg-Gal4;UAS-EcR-DN 0 hr dLipin No RT
w^{118} 6 hr Actin 5c RT	w^{118} 6 hr Actin 5c RT	w^{118} 6 hr Actin 5c RT	w^{118} 6 hr Actin 5c No RT	Blank	Blank	Blank	Blank	cg-Gal4;UAS-EcR-DN 6 hr Actin 5c RT	cg-Gal4;UAS-EcR-DN 6 hr Actin 5c RT	cg-Gal4;UAS-EcR-DN 6 hr Actin 5c RT	cg-Gal4;UAS-EcR-DN 6 hr Actin 5c No RT
w^{118} 6 hr dLipin RT	w^{118} 6 hr dLipin RT	w^{118} 6 hr dLipin RT	w^{118} 6 hr dLipin No RT	Blank	Blank	Blank	Blank	cg-Gal4;UAS-EcR-DN 6 hr dLipin RT	cg-Gal4;UAS-EcR-DN 6 hr dLipin RT	cg-Gal4;UAS-EcR-DN 6 hr dLipin RT	cg-Gal4;UAS-EcR-DN 6 hr dLipin No RT
w^{118} 12 hr Actin 5c RT	w^{118} 12 hr Actin 5c RT	w^{118} 12 hr Actin 5c RT	w^{118} 12 hr Actin 5c No RT	Blank	Blank	Blank	Blank	cg-Gal4;UAS-EcR-DN 12 hr Actin 5c RT	cg-Gal4;UAS-EcR-DN 12 hr Actin 5c RT	cg-Gal4;UAS-EcR-DN 12 hr Actin 5c RT	cg-Gal4;UAS-EcR-DN 12 hr Actin 5c No RT
w^{118} 12 hr dLipin RT	w^{118} 12 hr dLipin RT	w^{118} 12 hr dLipin RT	w^{118} 12 hr dLipin No RT	Blank	Blank	Blank	Blank	cg-Gal4;UAS-EcR-DN 12 hr dLipin RT	cg-Gal4;UAS-EcR-DN 12 hr dLipin RT	cg-Gal4;UAS-EcR-DN 12 hr dLipin RT	cg-Gal4;UAS-EcR-DN 12 hr dLipin No RT

LITERATURE CITED

An, P. N. T., Yamaguchi, M., & Fukusaki, E. (2017). Metabolic profiling of *Drosophila melanogaster* metamorphosis: a new insight into the central metabolic pathways. Metabolomics, 13, 1-13.

Arquier, N., & Léopold, P. (2007). Fly foie gras: modeling fatty liver in *Drosophila*. Cell Metabolism, 5(2), 83-85.

Baker, K. D., & Thummel, C. S. (2007). Diabetic larvae and obese flies—emerging studies of metabolism in *Drosophila*. Cell metabolism, 6(4), 257-266.

Brand, A. H., & Perrimon, N. (1993). Targeted gene expression as a means of altering cell fates and generating dominant phenotypes. development, 118(2), 401-415.

Britton, J. S., Lockwood, W. K., Li, L., Cohen, S. M., & Edgar, B. A. (2002). *Drosophila's* insulin/PI3-kinase pathway coordinates cellular metabolism with nutritional conditions. Developmental cell, 2(2), 239-249.

Colombani, J., Bianchini, L., Layalle, S., Pondeville, E., Dauphin-Villemant, C., Antoniewski, C., Carré, C., Noselli, S., & Léopold, P. (2005). Antagonistic actions of ecdysone and insulins determine final size in *Drosophila*. Science, 310(5748), 667-670.

Colombani, J., Raisin, S., Pantalacci, S., Radimerski, T., Montagne, J., & Léopold, P. (2003). A Nutrient Sensor Mechanism Controls *Drosophila* Growth. Cell, 114(6), 739–749. https://doi.org/10.1016/S0092-8674(03)00713-X

Csaki, L. S., & Reue, K. (2010). Lipins: multifunctional lipid metabolism proteins. Annual review of nutrition, 30, 257-272.

Duffy, J. B. (2002). *GAL4* system in *Drosophila*: a fly geneticist's Swiss army knife. genesis, 34(1-2), 1-15.

Fernández-Moreno, M. A., Farr, C. L., Kaguni, L. S., & Garesse, R. (2007). *Drosophila melanogaster* as a model system to study mitochondrial biology. Mitochondria: Practical Protocols, 33-49.

Grewal, S. S. (2012). Controlling animal growth and body size–does fruit fly physiology point the way?. F1000 biology reports, 4.

Han, S., Bahmanyar, S., Zhang, P., Grishin, N., Oegema, K., Crooke, R., ... & Goodman, J. M. (2012). Nuclear envelope phosphatase 1-regulatory subunit 1 (formerly TMEM188) is the metazoan Spo7p ortholog and functions in the lipin activation pathway. *Journal of Biological Chemistry*, 287(5), 3123-3137.

Harris, T. E., & Finck, B. N. (2011). Dual function lipin proteins and glycerolipid metabolism. Trends in Endocrinology & Metabolism, 22(6), 226-233.

Heier, C., & Kühnlein, R. P. (2018). Triacylglycerol metabolism in *Drosophila melanogaster*. Genetics, 210(4), 1163-1184.

Hood, S. E., Kofler, X. V., Chen, Q., Scott, J., Ortega, J., & Lehmann, M. (2020). Nuclear translocation ability of Lipin differentially affects gene expression and survival in fed and fasting *Drosophila*. Journal of lipid research, 61(12), 1720–1732. https://doi.org/10.1194/jlr.RA120001051

Kamoshida, Y., Fujiyama-Nakamura, S., Kimura, S., Suzuki, E., Lim, J., Shiozaki-Sato, Y., Kato, S., & Takeyama, K. I. (2012). Ecdysone receptor (EcR) suppresses lipid accumulation in the *Drosophila* fat body via transcription control. Biochemical and biophysical research communications, 421(2), 203-207.

Kannangara, J. R., Mirth, C. K., & Warr, C. G. (2021). Regulation of ecdysone production in *Drosophila* by neuropeptides and peptide hormones. *Open Biology*, *11*(2), 200373.

Koyama, T., Texada, M. J., Halberg, K. A., & Rewitz, K. (2020). Metabolism and growth adaptation to environmental conditions in *Drosophila*. Cellular and Molecular Life Sciences, 77(22), 4523-4551.

Lehmann, M. (2018). Endocrine and physiological regulation of neutral fat storage in *Drosophila*. Molecular and cellular endocrinology, 461, 165-177.

Malita, A., & Rewitz, K. (2021). Interorgan communication in the control of metamorphosis. Current opinion in insect science, 43, 54-62.

Merkey, A. B., Wong, C. K., Hoshizaki, D. K., & Gibbs, A. G. (2011). Energetics of metamorphosis in *Drosophila melanogaster*. Journal of insect physiology, 57(10), 1437-1445.

Nelliot, A., Bond, N., & Hoshizaki, D. K. (2006). Fat-body remodeling in *Drosophila melanogaster*. genesis, 44(8), 396-400.

Notarangelo, G. (2014). *The Role of βFTZ-F1 and MMP2 in Regulating Hormone-Mediated Autophagy and Insulin Signaling in the Drosophila Fat Body.* Mount Holyoke College.

Peterson, T. R., Sengupta, S. S., Harris, T. E., Carmack, A. E., Kang, S. A., Balderas, E., Guertin, D. A., Madden, K. L., Carpenter, A. E., Finck, B. N., & Sabatini, D. M. (2011). mTOR complex 1 regulates *lipin-1* localization to control the SREBP pathway. Cell, 146(3), 408-420.

Pfaffl, M. W. (2001). A new mathematical model for relative quantification in real-time RT–PCR. *Nucleic acids research*, *29*(9), e45-e45.

Phan, J., & Reue, K. (2005). Lipin, a lipodystrophy and obesity gene. Cell metabolism, 1(1), 73-83.

Reue, K., & Dwyer, J. R. (2009). Lipin proteins and metabolic homeostasis. Journal of lipid research, 50, S109-S114.

Reue, K., & Zhang, P. (2008). The lipin protein family: dual roles in lipid biosynthesis and gene expression. FEBS letters, 582(1), 90-96.

Rusten, T. E., Lindmo, K., Juhász, G., Sass, M., Seglen, P. O., Brech, A., & Stenmark, H. (2004). Programmed autophagy in the *Drosophila* fat body is induced by ecdysone through regulation of the PI3K pathway. Developmental cell, 7(2), 179-192.

Schmitt, S., Ugrankar, R., Greene, S. E., Prajapati, M., & Lehmann, M. (2015). *Drosophila* Lipin interacts with insulin and TOR signaling pathways in the control of growth and lipid metabolism. Journal of cell science, 128(23), 4395–4406. https://doi.org/10.1242/jcs.173740

Thummel, C. S. (1996). Flies on steroids—*Drosophila* metamorphosis and the mechanisms of steroid hormone action. Trends in Genetics, 12(8), 306-310.

Ugrankar, R., Liu, Y., Provaznik, J., Schmitt, S., & Lehmann, M. (2011). Lipin is a central regulator of adipose tissue development and function in *Drosophila melanogaster*. Molecular and cellular biology, 31(8), 1646-1656.

White, K. P., Hurban, P., Watanabe, T., & Hogness, D. S. (1997). Coordination of *Drosophila* metamorphosis by two ecdysone-induced nuclear receptors. Science, 276(5309), 114-117.

Woodard, C. T., Baehrecke, E. H., & Thummel, C. S. (1994). A molecular mechanism for the stage specificity of the *Drosophila* prepupal genetic response to ecdysone. Cell, 79(4), 607-615.

Yamanaka, N., Rewitz, K. F., & O'Connor, M. B. (2013). Ecdysone control of developmental transitions: lessons from *Drosophila* research. Annual review of entomology, 58, 497-516.

Zhang, H., Stallock, J. P., Ng, J. C., Reinhard, C., & Neufeld, T. P. (2000). Regulation of cellular growth by the *Drosophila* target of rapamycin dTOR. Genes & development, 14(21), 2712-2724.